

Incremental Bootstrapping and Classification of Structured Scenes in a Fuzzy Ontology

Luca Buoncompagni^{ID} and Fulvio Mastrogiovanni^{ID}

Abstract—We foresee robots that bootstrap knowledge representations and use them for classifying relevant situations and making decisions based on future observations. Particularly for assistive robots, the bootstrapping mechanism might be supervised by humans who should not repeat a training phase several times and should be able to refine the taught representation. We consider robots that bootstrap structured representations to classify some intelligible categories. Such a structure should be incrementally bootstrapped, *i.e.*, without invalidating the identified category models when a new additional category is considered. To tackle this scenario, we presented the Scene Identification and Tagging (SIT) algorithm, which bootstraps structured knowledge representation in a crisp OWL-DL ontology. Over time, SIT bootstraps a graph representing scenes, sub-scenes and similar scenes. Then, SIT can classify new scenes within the bootstrapped graph through logic-based reasoning. However, SIT has issues with sensory data because its crisp implementation is not robust to perception noises. This paper presents a reformulation of SIT within the fuzzy domain, which exploits a fuzzy DL ontology to overcome the robustness issues. By comparing the performances of fuzzy and crisp implementations of SIT, we show that fuzzy SIT is robust, preserves the properties of its crisp formulation, and enhances the bootstrapped representations. On the contrary, the fuzzy implementation of SIT leads to less intelligible knowledge representations than the one bootstrapped in the crisp domain.

Index Terms—Incremental Knowledge Bootstrapping, Fuzzy Description Logic, Learn Structured Categories, Human-Robot Interaction.

I. INTRODUCTION

ROBOTS need representations concerning the environment and the tasks to be performed. Such representations are usually based on geometrical primitives applied to sensor data. However, when the robot interacts with humans, it should be aware of common human semantics [1], and it should also allow users to access and refine knowledge [2]. Crisp *ontologies* have been widely used for semantic representation and human intelligibility based on symbolic structures [3] but they are affected by robustness issues, since ontological concepts require perfect semantic relations [4], and this is particularly relevant when noisy sensory data are considered.

L. Buoncompagni and F. Mastrogiovanni are affiliated with the Department of Informatics, Bioengineering, Robotics and Systems Engineering, University of Genoa, Via Opera Pia 13, 16145, Genoa, Italy.

Corresponding author: luca.buoncompagni@edu.unige.it.

We thank Professor Alessandro Saffiotti, affiliated with the University of Örebro in Sweden, to have supported us with the theoretical foundation of the fuzzy logic approach developed in this manuscript.

We also thank Professor Umberto Straccia, affiliated with the National Research Council of Italy, for his hints and software tools to validate our approach.

Manuscript published the 17th April 2024.

Moreover, knowledge *bootstrapping* [5], which brings the gap between semantic concepts and models learning, and knowledge *grounding* [6], which allows symbolic representation to dealing with sensors, are challenging open issues.

We assume a scenario where the robot observes scenes and bootstraps a structured and intelligible representation used to classify similar scenes in the future. In particular, we focus on (i) an *incremental* learning approach to allow robots bootstrapping their representations while interacting with the environment and humans. Also, we aim to bootstrap (ii) *intelligible* representations since they would be suitable for human-robot interaction, especially when humans need to supervise the robot. To enable the classification of *similar* scenes and reasoning algorithms for actuating the robot, we want to bootstrap (iii) *structured* representations involving hierarchies that relates observed scenes to each other.

With these three objectives, we previously developed the Scene Identification and Tagging algorithm (SIT) [7], which exploits the Ontology Web Language (OWL) based on the Description Logic (DL) formalism [8]. Over time, SIT bootstraps scene categories in an ontology from observations, and it classifies future scenes within a graph of scenes previously observed. As detailed in Section II-B, SIT has limitations, some of which are addressed through the fuzzy formalisation of SIT that this paper presents. As detailed in Section II-C, this paper focuses on an extensions of SIT that is robust to noisy inputs and vague scenes, which could not be handled with the crisp formalisation of SIT previously proposed.

Section II presents the related work, our motivations, and contributions based on previous work. Section III introduces the formalism involved in a fuzzy ontology, and Section IV proposes the fuzzy extension of SIT. Section V shows experimental results, which lead to the discussions in Section VI.

II. BACKGROUND

A. Related Work

As surveyed in [9]–[11], machine learning techniques (*e.g.*, Deep Convolutional Neural Network) have been largely used to classify objects and scenes in support of tasks planning. These techniques effectively processing raw data, deal with perception noise, and learn generalised classifiers. The typical outcomes of such classifiers is a synthetic description of an image (or based on multimodal sensors) made by semantic labels. Since these labels are usually not structured, they do not provide a sophisticated representation to reason on the relations between elements in the scenes and among different scenes, which is relevant for task planning. However, there

are few work also addressing structured outcomes, *e.g.*, [12]. Machine learning have also be used in an incremental fashion, but the *catastrophic forgetting* [13] is still a challenging open issue, which occur when the overall performance of the classifier decreases due to the introduction of new types of scenes to be classified. This issue is even more relevant in our scenario, since a human supervisor should bootstrap the robot knowledge for the service of task planning with a few demonstrations. Moreover, machine learning approaches generate models that are usually not intelligible, and this limits the possibility of the human to supervise the robot knowledge. Although some learning techniques generate intelligible classifiers by design, their performances are typically lower than other approaches generating black-box like classifiers. Nonetheless, the problem of having explainable models have been addressed either with metrics that help understanding the reasons of a certain outcome, and by coupling machine learning with logic-based symbolic knowledge representation [14].

Symbolic learners have been developed to bootstrap, align or refine the concepts represented in OWL ontologies. For instance, [15] presents a method to generate ontologies from relational database, and gain the benefits of OWL reasoning. The Inductive Logic Programming [16] involves machine learning mechanisms to induce logic programs by generalising annotated datasets, also within ontological representations, *e.g.*, [17]. Decision Trees and Random Forests have been proposed to learn the representation of symbols in an ontology [18], while approaches based on kernels have been used in [19], on Naive Bayes in [20], on Genetic Programming in [21], and on Reinforcement Learning [22]. In addition, [23] proposes an approach to mind OWL cardinality restrictions.

Fuzzy OWL ontologies extends the OWL formalism with fuzzy degrees [24], and they require specific reasoners to deal with vague logic axioms, *e.g.*, the FuzzyDL reasoner [25], FIRE [26], Delorean [27], GURDL [28], GERDS [29], Soft-Facts [30], and LiFR [31]. Learners has been developed based on the FuzzyDL reasoner involving the identification of data types [32], and concepts inclusions [33]. Fuzzy ontologies have been also developed for spatial reasoning [34], object detection [35], and event recognition [36]. Learners based on fuzzy logic that do not rely on OWL ontologies have been proposed, *e.g.*, Deep Neural Networks have been coupled with fuzzy theories to improve the performances [37], and intelligibility issues have been also considered, *e.g.*, [38]. In contrast, crisp OWL ontologies have been also used to support probabilistic learners [39].

Although learning approaches that exploits logic-based symbolic formalisms (*e.g.*, crisp or fuzzy OWL ontologies) provided some degree of intelligibility and structured outcomes by design, we are not aware of approaches that incrementally bootstrap environmental models from observation over time. Instead, to bootstrap logic models, symbolic learning approaches rely on annotated datasets processed through a not incremental training phase, *i.e.*, if the dataset is augmented, then the training phase should be performed again to avoid catastrophic forgetting.

B. Crisp SIT Overview

We previously developed the crisp SIT algorithm [7], which encompass the *encoding*, *learning*, *structuring* and *classification* phases. As inputs, SIT requires symbolic facts f_i that represent the scene through *relations* r_z between pairs of *elements* (γ_x, γ_y) having relative *types* (Γ_s, Γ_h) . Figure 1 shows an example of input facts involving spatial relations r and objects shapes Γ , which constitute the SIT *input interface*, *i.e.*, the prior knowledge encoded in the ontology.

In the encoding phase, SIT maps facts into *beliefs*, which represent the currently observed *scene* as an OWL *instance* ϵ_t in the ontology. Beliefs are characterised by *cardinalities* c_{zsh} that describe the features of a scene through combinations of z -th relations and sh -th types, *e.g.*, “2 cups in front of a glass”.

The learning phase occurs when SIT cannot classify an encoded scene with high degree. In this phase, SIT learns a scene *category* Φ_t , which is stored as a new OWL *concept* in the ontology. Categories are defined through cardinality *restrictions* Ω , which are stored in the ontology for future classifications based on the the beliefs observed at a certain time instant. Then, SIT performs the structuring phase, which exploits DL-based reasoning to arrange the categories learned over time in a *memory graph* M . The memory is a hierarchy describing sub-scenes and their similarity through logic implications. We consider that SIT bootstrap knowledge when categories has been learned and structured in the memory.

Given input facts and the memory bootstrapped in the ontology, SIT exploits DL-based reasoning to perform the classification phase and provide a *classification graph* M_t^* . The latter is a sub-graph of M that only contains the bootstrapped categories concerning the input scene being classified (*i.e.*, the categories having cardinality restrictions *satisfied* by scene beliefs) at a certain time t . Each node of M_t^* might classify only a part of the scene (*i.e.*, a sub-scene), and this fact is measured through a *similarity* value $d_{\epsilon_t}^{\Phi_j}$, which is associate to each j -th categories in M_t^* .

It is noteworthy that SIT performs one-shot unsupervised learning of scene categories, which can be *incrementally* added in the ontology since a new category do not require to retrain the models of the previous learned categories. SIT bootstraps a *structured* set of categories that relates scenes having common parts. Also, SIT provides a classification based on semantic symbols, which are *intelligible* under some degree of intuitiveness. The classification accuracy and the intelligibility degree that characterise the bootstrapped representation depends on the used input interface. Such an interface makes SIT general in terms of scenes semantics, but it need to be carefully designed for each application.

The crisp implementation of SIT is computationally complexity since it uses DL reasoning processes for structuring the memory and classifying scenes. Indeed, the reasoning process is exponentially complex with respect to the number of axioms involved in the ontology [8], which depends on the number of symbols encoded in the input interface, and on the number of categories learned in the ontology. Furthermore, SIT learns a category for each scene that it is not able to classify with a high degree. This behaviour does not lead to *overfitting*, *i.e.*, SIT

would not misclassify the scene, but it would provide a more complex classification involving several similar scenes, and this would affect the computation load. Although Section V-E presents the computation complexity of the fuzzy SIT, this paper does not focus on the computation issues specifically. Nonetheless, Section VI discusses the approaches we are considering to overcome these issues.

Another issue of the crisp SIT concerns the *robustness* of M and M_t^* with respect to noisy and vague inputs facts. Indeed, learned categories are defined through cardinality restrictions involving crisp threshold-based rules, which might be satisfied (or not) based on beliefs cardinalities. Thus, small errors in the perception of the beliefs might lead to very different categories bootstrapped in the memory M and, consequently, to different classification outcomes M_t^* . To overcome this limitation in the crisp domain, we exploited the intelligibility of the bootstrapped categories and the possibility to refine them without the need to retrain all the learned categories. In [40], we presented an architecture where a human verbally interacts with the robot to supervise if cardinality beliefs have been correctly perceived, but this approach demands high effort from the human. Through the fuzzy extension of SIT presented in this paper, we aim to overcome the robustness issues and make the data supervision mechanism optional.

C. Contribution

This paper presents the fuzzy SIT algorithm¹, which is an extension of the crisp SIT based on a fuzzy ontology subjected to the inferences computed by the FuzzyDL reasoner. Our objective is to preserve the characteristic of the crisp implementation of SIT, while allowing for a fuzzy representation of beliefs cardinalities and restrictions. Hence, we aim to improve the robustness of SIT by not considering discontinuities in the identification of satisfied cardinality restrictions, as it occurs in the crisp domain. In other words, we aim for a smooth transition between bootstrapped scenes representation such to have consistent models even when inputs facts are noisy.

In a previous work, we preliminary introduced the fuzzy SIT algorithm [41] while, in this paper we detail its theoretical foundations, and how it extends its crisp counterpart. Also, we present experimental results showing that fuzzy SIT improves robustness while having a behaviour consistent with the crisp domain. Differently from the crisp SIT, fuzzy SIT represents vague scenes with fuzzy relations and elements having more than one *type*. Such a vague representation allows using input facts that are retrieved from sensors with more sophisticated mechanisms than crisp thresholds. In addition, fuzzy SIT introduces fuzzy classification and implication degrees, which enrich the bootstrapped memory and the relative classification graphs.

Although fuzzy SIT bootstraps more expressive and robust representations than crisp SIT, the latter learns and classifies scenes within a more intelligible representation. Hence, further work is required for making fuzzy SIT being as much intuitive to human as in the crisp domain. Another drawback we assess through experiments concerns the scene similarities measure,

Table I
THE DESCRIPTION LOGIC FORMALISM USED IN THIS PAPER.

CONCEPT	Capital Greek letter, <i>e.g.</i> , Δ, Φ, Γ , <i>etc.</i>
role	Bold letter, <i>e.g.</i> , $\mathbf{r}, \mathbf{p}, \mathbf{q}$, <i>etc.</i>
Instance	Greek letter, <i>e.g.</i> , α, β, γ , <i>etc.</i>
$\Delta \sqsubseteq \Phi$	Δ is a <i>sub-concept</i> of Φ , <i>i.e.</i> , Δ implies Φ .
$\alpha:\Delta$	The instance α is <i>classified</i> in the Δ concept.
$(\alpha, \beta):\mathbf{r}$	The α instance is <i>related</i> with the \mathbf{r} role to the β instance.
$\Delta \triangleq \mathcal{R} \mathbf{r} \Phi$	Define Δ to classify instances α with \mathbf{r} spanning in $\beta:\Phi$. The <i>cardinality restriction</i> \mathcal{R} can be: <i>some</i> , <i>only</i> , <i>exact</i> $\min c$ or $\max c$, <i>i.e.</i> , $\{\exists, \forall, =, \geq, \leq\}$, $c \in \mathbb{N}^+$.
$\Delta \triangleq \Phi \sqcap \Pi$	Define Δ as the <i>conjunction</i> of Φ and Π .
$\Delta \triangleq \Phi \sqcup \Pi$	Define Δ as the <i>disjunction</i> of Φ and Π .

which is bounded in $[0, 1]$ for crisp SIT, while it is bounded in a range that depends on the application setups for fuzzy SIT.

III. OWL ONTOLOGY AND FUZZY DL PRIMER

An OWL ontology is a collection of logic *axioms*, which relate *symbols* to represent *things* in the DL formalism. An OWL *reasoner* infers symbolic *hierarchies* by checking if the axioms are logically consistent. The reasoner adheres to the *open word* assumption, which assumes that the truthfulness of an axiom is independent of whether or not the related symbols are known. The DL symbols that occur in ontological axioms are: *concepts* (or classes), *instances* (or individuals), and *roles* (or properties); as shown in Table I.

Concepts are structured in a graph of logic implications, while instances are classified into concepts by the mean of roles, which relate pairs of either instances or concepts. Table I also summarises the notation we used for generic representations (*e.g.*, a concept Γ), and its name as encoded in an OWL ontologies (*e.g.*, the SPHERE concept). The OWL formalism also specifies *concrete concepts* (*e.g.*, the data type \mathbb{R}), classifying special types of instances (*e.g.*, numbers) that can be related to the other instances through *concrete roles*.

An Ontology collects *axioms* \mathcal{A}_i , which define symbols and their logic-based semantics. Table I details the axioms relevant for this paper, *e.g.*, SPHERE \sqsubseteq SHAPE (*i.e.*, sphere is a type of shape), Sp1:SPHERE (*i.e.*, Sp1 is a sphere), (Sp1,0.2):hasRadius (*i.e.*, Sp1 has radius 0.2m), and SPHERE \triangleq =1 hasRadius.METER (*i.e.*, each sphere has exactly one radius). Also, concepts can be defined as the conjunction (*i.e.*, \sqcap), or disjunction (*i.e.*, \sqcup), of other concepts. Refer to [8] and [42] for details about crisp OWL-DL axioms.

In a fuzzy ontology, some axioms are paired with a fuzzy degree $\langle \mathcal{A}_i, p^{\mathcal{A}_i} \rangle$, with $p^{\mathcal{A}_i} \in \mathbb{R}^{[0,1]}$ *e.g.*, $p^{\Delta \sqsubseteq \Phi} p^{\alpha:\Delta}$, or $p^{(\alpha,\beta):\mathbf{r}}$. Other axioms, such as the one concerning concept definition, their conjunctions and disjunction (*e.g.*, $\Delta \triangleq \exists \mathbf{r}.\Phi$, $\Phi \sqcap \Pi$ and $\Phi \sqcup \Pi$), are paired with a fuzzy *membership* functions, which spans in $[0, 1]$; *e.g.*, Figure 2a.

The FuzzyDL reasoner evaluates fuzzy axioms to infer implicit axioms and resolve queries with different logics [43], and we used the Zaden logic. The classification phase of SIT exploits the implicit axioms concerning the classification of instances into concepts (*e.g.*, $\alpha:\Delta$), while the structuring phase relies on the assessments of concepts implications for retrieving a graph of concepts (*e.g.*, $\Delta \sqsubseteq \Phi$).

¹Available at https://github.com/buoncubi/fuzzy_sit.

Noteworthy, FuzzyDL cannot reason on *cardinality restriction axioms* $\Delta \triangleq \geq c r. \Phi$, (e.g., $\Delta \triangleq \geq 2 \text{ contain. BALL}$). In a crisp ontology, this type of axioms defines a concept Δ classifying instances α that are involved in *at least* (i.e., \geq) $c \in \mathbb{N}^+$ roles $(\alpha, \beta):r$, with different instances β classified in the Φ concept. For example, an instance $\alpha \equiv \text{Supplier}$ would be classified as $\alpha:\Delta$ if the ontology encodes at least the axioms: $(\alpha, \beta_1):\text{contain}$, $\beta_1:\text{BALL}$, and $(\alpha, \beta_2):\text{contain}$, $\beta_2:\text{BALL}$.

More generally, FuzzyDL cannot reason on the exact, min and max crisp cardinality restrictions (introduced in Table I) because the problem of counting fuzzy elements is far from trivial [44]. Among several proposal [45], the σ -count is a popular approach defining the cardinality c as the sum of the fuzzy degrees of all the items in a set. This approach treats cardinality as a real positive number, i.e., $c \in \mathbb{R}^+$, and it computes the *energy* of a set, which is a cardinality measure assuming that the higher the energy value, the more items the fuzzy set should have. However, the σ -count cannot discriminate differences between a set having 10 items with fuzzy degree 0.1, or one item with degree equal to 1.

Since SIT is based on cardinality restriction axioms, we exploited the σ -count approach to compute fuzzy cardinalities c , which are stored in the ontology as numbers related to an instance ϵ_t through a concrete role r , i.e., $(\epsilon_t, c):r$. Then, we implement a cardinality restriction through a *left-shoulder* membership function Ω applied to a concrete concept in the ontology (i.e., a fuzzy set, as shown in Figure 2a), and we define a concept $\Phi \triangleq \exists r. \Omega$. Hence, ϵ_t would be classified in Φ , and the relative fuzzy degree $p^{\epsilon_t:\Phi}$ would be computed, if the cardinality c satisfied the Ω restriction. In other words, we classify the instance ϵ_t based on the fuzzy membership value of c in Ω , as more detailed in Sections IV-C, IV-D, and IV-E. This approach allow defining fuzzy cardinality restrictions that are satisfied based on a continuous membership distribution Ω . In contrast, crisp cardinality restrictions relies on thresholds, which lead to robustness issues due to discontinuities.

IV. THE FUZZY SIT ALGORITHM

A. The Input Interface

SIT defines scenes made of some *elements* γ_j that are represented through prior knowledge concerning their *types* Γ and *relations* r . In particular, elements of a scene have fuzzy membership degrees in some of the types $\{\Gamma_1, \dots, \Gamma_v\} \subseteq \Gamma$, and their might be paired by fuzzy relations $\{r_1, \dots, r_w\} \subseteq r$.

SIT requires input *facts* $F_t = \{f_1, \dots, f_n\}$, which describe a scene at a certain time instant t . Each fact f_i specifies a relation between two elements, i.e., $(\gamma_x, \gamma_y):r_z$, taking also into account the types of the x -th and y -th elements. We denote with $\Gamma^x \subseteq \Gamma$ and $\Gamma^y \subseteq \Gamma$ the types of the two elements, i.e., $\gamma_x:\Gamma_s, \forall \Gamma_s \subseteq \Gamma^x$, and $\gamma_y:\Gamma_h, \forall \Gamma_h \subseteq \Gamma^y$. Thus, given fuzzy degrees $p_{iz} \triangleq p^{(\gamma_x, \gamma_y):r_z}$, $p_{is} \triangleq p^{\gamma_x:\Gamma_s}$, and $p_{ih} \triangleq p^{\gamma_y:\Gamma_h}$, a fact f_i is defined in the ontology as:

$$f_i = \left\{ \langle (\gamma_x, \gamma_y):r_z, p_{iz} \rangle; \left\{ \langle \gamma_x:\Gamma_s, p_{is} \rangle, \forall \Gamma_s \subseteq \Gamma^x \right\}; \left\{ \langle \gamma_y:\Gamma_h, p_{ih} \rangle, \forall \Gamma_h \subseteq \Gamma^y \right\} \right\}. \quad (1)$$

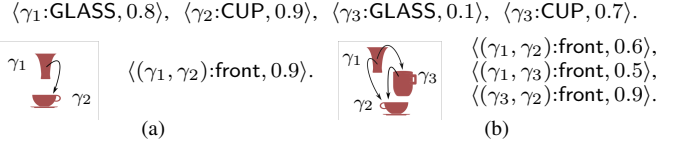


Figure 1. Examples of input *facts* that represent two *scenes*. The description of the elements types (on top) is in common for both scenes.

The *input interface* (1) allows using SIT with general-purpose combinations of symbols that imply Γ or r , which semantics might be further specified in the ontology. As an example, Figure 1 shows some facts based on prior knowledge involving $\Gamma \supseteq \{\text{CUP}, \text{GLASS}\}$, and $r \supseteq \{\text{front}\}$, i.e., $v = 2$ and $w = 1$.

Since an element that occurs in different relation always has the same type, we could simplify F_t by removing the axioms concerning Γ_s and Γ_h that are duplicated in different f_i . Hence F_t can be considered as a collection of two sets: one concerns the types of each element $\gamma_j:\Gamma_j$ (e.g., as shown on top of Figure 1), and the other represents the relations between elements $(\gamma_x, \gamma_y):r_z$ (e.g., as shown on Figures 1a and 1b).

B. Encoding Phase

The encoding phase maps F_t into an OWL instance ϵ_t , which represents the *scene* at the current time instant t . Such an instance encodes in the ontology the features of a scene as combinations of *beliefs*, which are reification of facts. The *reify* operator $\mathcal{R}(r_z, \Gamma_s, \Gamma_h) \triangleq r_{zsh}$ defines a role through a concatenation of constituent symbols, e.g., $r_{zsh} \equiv \text{front GLASS CUP}$, which represents that some cups are in front of some glasses.

The crisp implementation of SIT exploits belief encoded in the ontology as $(\epsilon_t, \gamma_x):r_{zsh}$, and it classifies the scene ϵ_t based on *minimal cardinality restrictions*, i.e., by limiting the minimum number of beliefs for each zsh -th combination. However, as introduced in Section III, FuzzyDL cannot reason on cardinality restrictions, and we rely the σ -count approach to represent the cardinalities of the encoded beliefs.

Hence, fuzzy SIT associates beliefs to the facts in F_t as the conjunction of the zsh -th combinations occurring in (1), i.e.,

$$\langle (\gamma_x, \gamma_y):r_z, p_{iz} \rangle \sqcap \langle \gamma_x:\Gamma_s, p_{is} \rangle \sqcap \langle \gamma_y:\Gamma_h, p_{ih} \rangle. \quad (2)$$

Based on the DL Zadeh logic [43], the fuzzy degree of the axiom resulting from (2) is the minimum value among p_{iz} , p_{is} and p_{ih} . Thus, the *cardinality* of the zsh -th belief computed with the σ -count approach is

$$c_{zsh} = \sum_{f_i}^{F_t} \min\{p_{iz}, p_{is}, p_{ih}\} \in \mathbb{R}^+. \quad (3)$$

In the ontology, each zsh -th belief is represented with *concrete* crisp roles involving a scene instance ϵ_t , i.e., $\langle (\epsilon_t, c_{zsh}):r_{zsh}, 1 \rangle$. Beliefs are given by the *encoding function* \mathcal{E} , which pairs reified roles and fuzzy cardinalities as

$$\mathcal{E}(F_t) : \{ \langle r_{zsh}, c_{zsh} \rangle, \forall r_z \subseteq r; \forall \Gamma_s, \Gamma_h \subseteq \Gamma \} \triangleq B_t. \quad (4)$$

For example, the scene in Figure 1a is encoded through one belief, i.e., $B_t = \{ \langle \text{front GLASS CUP}, 0.8 \rangle \}$. Similarly, the set of beliefs B_t concerning Figure 1b is encoded in the ontology as

$(\epsilon_t, 1.2)$:front GLASS CUP, $(\epsilon_t, 0.1)$:front GLASS GLASS, and $(\epsilon_t, 0.7)$:front CUP CUP. Noteworthy, not all zsh -th combinations always occurs in B due to the open word assumption.

C. Learning Phase

The learning phase evaluates the beliefs of the current scene ϵ_t to generate minimum cardinality restrictions for classifying similar scenes in the future. Based on the σ -count approach applied to a fuzzy ontology, a minimum cardinality restriction is a *concrete* concept Ω that defines a fuzzy set with a *left-shoulder* membership function. As shown in Figure 2a, such a function maps a belief cardinality $c_{zsh} \in \mathbb{R}^+$ into a fuzzy degree $p_{zsh}^{\epsilon_t: \Phi_j}$, which contributes to the classification of future scenes as far as the zsh -th combination is concerned.

We parametrize such a membership function as ${}^a\Omega(k)$ where k is equal to the c_{zsh} cardinality that was encoded in ϵ_t at a certain time, and $a \in [0, 1]$ is the *fuzziness* value used to compute $k^- = k \cdot (1 - a)$. If $a=0$, Ω becomes a crisp cardinality restriction while, if $a=1$, a non zero degree would be assigned to all $c_{zsh} > 0$. Given ${}^a\Omega(k)$ generated in a previous time instant, and a cardinality value c_{zsh} related to the current scene ϵ_t , we would consider the minimal fuzzy restriction *satisfied* if $c_{zsh} \geq k$, *i.e.*, $p_{zsh} = 1$. Instead, when $c_{zsh} \leq k^-$, the restriction would be *not satisfied*, *i.e.*, $p_{zsh} = 0$, while if $c_{zsh} \in (k^-, k)$ then the restriction will be *fuzzy satisfied*, *i.e.*, $p_{zsh} \in (0, 1)$.

Given encoded beliefs B_t related to ϵ_t (4), the *learning function* \mathcal{L} defines a new scene *category* Φ_t that restricts each zsh -th combination occurring in B_t with a relative Ω . To define the learned categories as nodes of the memory graph, we pose $\Phi_t \sqsubseteq \Phi$, where Φ is a concept defined in the ontology as prior knowledge to represent the empty scene, *i.e.*, Φ is the root of the memory graph. Formally, \mathcal{L} allows learning categories Φ_t as conjunctions of cardinality restrictions, *i.e.*, $\exists \mathbf{r}_{zsh}. {}^a\Omega(c_{zsh})$ with a fuzzy degree equal to 1; namely,

$$\mathcal{L}(B_t, a) : \langle \Phi, 1 \rangle \prod_{zsh}^{B_t} (\exists \mathbf{r}_{zsh}. {}^a\Omega(c_{zsh}), 1) \triangleq \Phi_t. \quad (5)$$

For instance, given the beliefs of the scene shown in Figure 1a, SIT would learn a category Φ_t with the restriction $\exists \text{front GLASS CUP}. {}^a\Omega(0.8)$. As introduced in Section III, and coherently with the crisp implementation of SIT, such a restriction indicates that a future scene can be classified in Φ_t if “at least 0.8 cups are in front of glasses”. Similarly, the category learned from the scene shown in Figure 1b is

$$\begin{aligned} \Phi_t &\triangleq \Phi \sqcap \exists \text{front GLASS CUP}. {}^a\Omega(1.2) \sqcap \\ &\exists \text{front GLASS GLASS}. {}^a\Omega(0.1) \sqcap \exists \text{front CUP CUP}. {}^a\Omega(0.7). \end{aligned} \quad (6)$$

Since FuzzyDL respects the open word assumption, some zsh -th combination are unspecified in Φ_t , but they might occur in the beliefs of a future scene classified in the Φ_t category.

D. Structuring Phase

The structuring phase exploits the FuzzyDL reasoner to generate a memory graph M having previously learned categories as nodes (*e.g.*, Φ_1 , Φ_2 , *etc.*), while edges are based on fuzzy

subsumption axioms. In particular, a node in the graph Φ_2 that is a sub-scene category of Φ_1 is represented in the ontology with the subsumption axiom $\langle \Phi_2 \sqsubseteq \Phi_1, p^{\Phi_2 \sqsubseteq \Phi_1} \rangle$. Since we adopted the DL Zadeh logic [43], and since \mathcal{L} (5) defines a conjunction of restrictions, the subsumption degree $p^{\Phi_2 \sqsubseteq \Phi_1}$ is the minimum $p_{zsh}^{\Phi_2 \sqsubseteq \Phi_1}$ value among the zsh -th combinations restricted either by Φ_1 and Φ_2 . However, if a zsh -th combination occurs in Φ_1 but does not occur in Φ_2 , we consider $p^{\Phi_2 \sqsubseteq \Phi_1} = 0$. Instead, if a zsh -th combination occurs in Φ_2 but does not occur in Φ_1 , FuzzyDL relies on the open word assumption to disregard such a zsh -th combination while computing $p^{\Phi_2 \sqsubseteq \Phi_1}$.

For each categories pair (Φ_1, Φ_2) restricting the same zsh -th combination respectively with ${}^a\Omega_1(k_1)$ and ${}^a\Omega_2(k_2)$, FuzzyDL computes the $p_{zsh}^{\Phi_2 \sqsubseteq \Phi_1}$ degree as the minimum value of the membership function representing the implication $\Omega_2 \Rightarrow \Omega_1$. In particular, the $p_{zsh}^{\Phi_2 \sqsubseteq \Phi_1}$ degree is computed based on the three following situations. If $k_1^- \leq k_2^-$ (Figure 2b) the restriction Ω_2 will always *respects* Ω_1 , *i.e.*, $\Phi_2 \sqsubseteq \Phi_1$ with $p_{zsh}^{\Phi_2 \sqsubseteq \Phi_1} = 1$. When $k_2^- < k_1^- < k_2$ (Figure 2c) the restriction Ω_2 *fuzzy respects* Ω_1 , *i.e.*, $p_{zsh}^{\Phi_2 \sqsubseteq \Phi_1} \in (0, 1)$. When $k_2 < k_1^-$ (Figure 2d), the restriction Ω_2 does *not respect* Ω_1 , thus, $\Phi_2 \not\sqsubseteq \Phi_1$, *i.e.*, $p_{zsh}^{\Phi_2 \sqsubseteq \Phi_1} = 0$.

We map subsumption axioms in a partially ordered set M , which is an oriented weighted graph with a root node Φ . In M , the axiom $\Phi_2 \sqsubseteq \Phi_1$ would be represented as an edge departing from the child Φ_2 and entering in the parent Φ_1 with a weight $p^{\Phi_2 \sqsubseteq \Phi_1} > 0$; *i.e.*, an implication arrow, as shown in Figures 4f and 4g. A child node always restricts more beliefs than its parents, *i.e.*, the child categorises a more complex scene that contains its parents, which are sub-scenes.

For instance, if the fuzziness value a is such that the restriction learned from the belief $(\epsilon_2, 1.2)$:front GLASS CUP satisfies $(\epsilon_1, 0.8)$:front GLASS CUP with a degree $p_{121}^{\Phi_2 \sqsubseteq \Phi_1} = 0.9$, then the scene Φ_2 (shown in Figure 1b) would be a child of Φ_1 (shown in Figure 1a) with subsumption degree that involves a single zsh -th combination, *i.e.*, $p^{\Phi_2 \sqsubseteq \Phi_1} = \min\{p_{121}^{\Phi_2 \sqsubseteq \Phi_1}\}$.

We formally indicate the DL-based reasoning process to generate the *memory graph* M with the *structuring function* \mathcal{S} , which can be expressed in an incremental fashion as

$$\mathcal{S}(M_{t-1}, \Phi_t) : \{\Phi, \Phi_1, \Phi_2, \dots, \Phi_{t-1}, \Phi_t; \sqsubseteq\} \triangleq M_t. \quad (7)$$

Given a new category Φ_t , and an initial memory $M_0 = \{\Phi\}$, \mathcal{S} updates the edges of M_{t-1} to compute M_t . FuzzyDL performs \mathcal{S} , which results are retrieved by quering the subsumption degrees $p^{\Phi_t \sqsubseteq \Phi_j} \forall \Phi_l, \Phi_j \sqsubseteq \Phi$ with $l \neq j$.

E. Classification Phase

In the classification phase, SIT attempts to classify a scene ϵ_t within some nodes Φ_j of a memory graph M_t previously structured. A classification $\epsilon_t: \Phi_j$ occurs when all the $\mathbf{r}_{zsh}. {}^a\Omega(k)$ restrictions of Φ_j are satisfied² by the c_{zsh} cardinalities of ϵ_t encoded in the ontology (4). Since \mathcal{L} (5) defines conjunctions of cardinality restrictions, the *classification degree* $p^{\epsilon_t: \Phi_j}$ is the minimum $p_{zsh}^{\epsilon_t: \Phi_j}$ degree among all the zsh -th combinations

²Accordingly with the second paragraph of Section IV-C and Figure 2a.

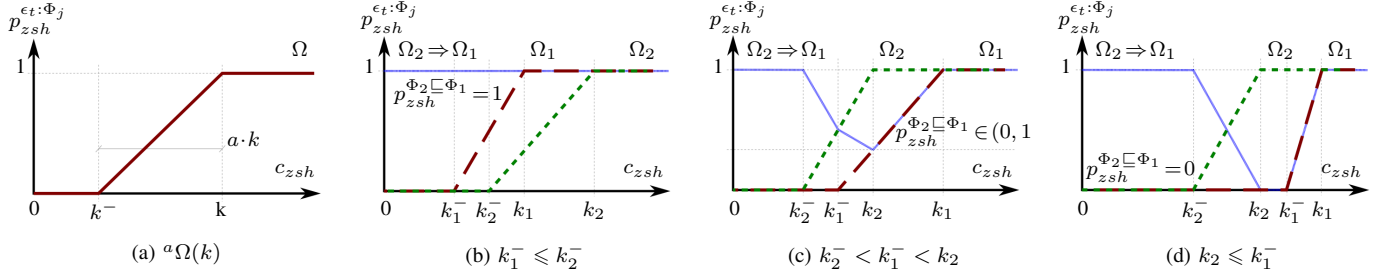


Figure 2. Figure (a) shows the membership function Ω , which defines a minimal *cardinality restriction* to k . Given a *fuzziness* value $a \in [0, 1]$ and a cardinality $c_{zsh} \in \mathbb{R}^+$, ${}^a\Omega(k)$ specifies the fuzzy degree $p_{zsh}^{\epsilon_t: \Phi_j}$ that represents if c_{zsh} satisfies the restriction. The other figures show two cardinality restrictions Ω_1 (in red) and Ω_2 (in green), which are associated to a zsh -th beliefs combination of the learned category Φ_1 and Φ_2 , respectively. Figures (b), (c) and (d) show the implication of Ω_1 and Ω_2 (in blue), which minimum value is the *subsumption degree* $p_{zsh}^{\Phi_1 \sqsubseteq \Phi_2}$, and it is used to identify implications between scenes categories, *i.e.*, the structure of bootstrapped knowledge into a graph. In particular, (b) shows the case where the minimal cardinality restriction Ω_2 always implies Ω_1 (*i.e.*, Ω_2 respects the restriction Ω_1), while (d) shows the case where Ω_2 never implies Ω_2 , and (c) show the case where the implication has a fuzzy degree in $(0, 1)$.

restricted by Φ_j . If $p^{\epsilon_t: \Phi_j} = 0$, we would consider the scene ϵ_t as not classified in Φ_j .

Given the structure of the memory graph M_t , the scene ϵ_t would be classified on its sub-graph because each parent of a classified category Φ_j also are classifications of ϵ_t , *i.e.*, sub-scenes. This sub-graph is named *classification graph* M_t^* and is given by the *classification function* \mathcal{C} , which is computed by FuzzyDL. The outcomes of \mathcal{C} are retrieved by querying all categories in M_t with a classification degree $p^{\epsilon_t: \Phi_j} > 0$, *i.e.*,

$$\mathcal{C}(M_t, B_t) : \{\forall \Phi_j \in M_t \mid p^{\epsilon_t: \Phi_j} > 0; \sqsubseteq\} \triangleq M_t^*. \quad (8)$$

The crisp implementation of SIT defines the *similarity* value to discriminate categories that are classified based on few restrictions. Indeed, M_t^* might involve a category with classification degree $p^{\epsilon_t: \Phi_j} = 1$ even if ϵ_t is more complex than Φ_j , *i.e.*, ϵ_t has higher cardinalities and more beliefs than Φ_j , which classifies only a small sub-scene of ϵ_t . Analogously, the fuzzy similarity $d_{\epsilon_t}^{\Phi_j}$ can be defined as the ratio between the zsh -th restrictions of Φ_j and the c_{zsh} cardinalities of ϵ_t

$$d_{\epsilon_t}^{\Phi_j} \triangleq \frac{d^{\Phi_j}}{d_{\epsilon_t}} = \frac{\sum_{\mathbf{r}_{zsh}}^{\Phi_j} k_{zsh}}{\sum_{\mathbf{r}_{zsh}}^{B_t} c_{zsh}}. \quad (9)$$

In the crisp case, $d_{\epsilon_t}^{\Phi_j} \in [0, 1]$ since $d_{\epsilon_t} \geq d^{\Phi_j}$, otherwise, Φ_j would not be a node of M_t^* because its restrictions would not be satisfied. In the fuzzy domain, the similarity is still bounded but it might be bigger than 1 when c_{zsh} is within the range defined by the fuzziness parameter a . As shown in Figure 8 (presented in Section V), the more the similarity exceeds 1, the lower $p^{\epsilon_t: \Phi_j}$ becomes. Moreover, the fuzzy similarity value $d_{\epsilon_t}^{\Phi_j}$ is not linear with the number of scene elements but with the number of input facts; consistently with the crisp domain.

For instance, the scene ϵ_2 encoded from Figure 1b would be classified in the category Φ_1 learned from Figure 1a with a degree $p^{\epsilon_2: \Phi_1} = 1$ because the front GLASSCUP belief of the scene satisfies the restriction of the category. However, since some of the scene beliefs are not restricted by the classifying category, the similarity value would be $d_2^1 = 0.8/2$.

It is noteworthy that SIT provides an expressive data structure M_t^* . Indeed, M_t^* inherits from M_{t-q} the cardinality restrictions (5) associated to each category classifying a scene ϵ_t ,

and the subsuming degree $p^{\Phi_i \sqsubseteq \Phi_j}$ between the relative nodes. In addition, each node of M_t^* also encodes a classification degree $p^{\epsilon_t: \Phi_j}$ and a similarity value $d_{\epsilon_t}^{\Phi_j}$, which measure how well the restrictions of a category satisfy scene beliefs, and how many beliefs are satisfied by that category, respectively.

F. Complexity Reduction

The scene features that SIT represents in the ontology span in a number of reified relation \mathbf{r}_{zsh} equal to $w \cdot v^2$, *i.e.*, all the combinations between a relation \mathbf{r} and two element types Γ (1). Since DL encompass the open word assumption, the number of axioms subjected to reasoning is typically reduced. However, DL reasoning is exponentially complex with the amount of axioms in the ontology. Hence, the computation performances are affected by w , v and the number of categories in M .

To reduce the complexity of SIT, we can change the reification operator presented in Section IV-B into $\mathcal{R}(\mathbf{r}_z, \Gamma_h) \triangleq \mathbf{r}_{zh}$, which defines beliefs involving a generic element type, *e.g.*, some cups are in front of some *objects*, *i.e.*, frontCUP. In this case, a belief that was defined in (2) becomes,

$$\bigsqcup_{\forall \Gamma_s \sqsubseteq \Gamma^x} \left\{ \langle (\gamma_x, \gamma_y) : \mathbf{r}_z, p_{iz} \rangle \sqcap \langle \gamma_x : \Gamma_s, p_{is} \rangle \sqcap \langle \gamma_y : \Gamma_h, p_{ih} \rangle \right\}, \quad (10)$$

and its cardinality, computed as in (3), becomes

$$c_{zh} = \sum_{f_i}^F \max_{\forall \Gamma_s \sqsubseteq \Gamma^x} \left\{ \min \{ p_{iz}, p_{is}, p_{ih} \} \right\}. \quad (11)$$

In this way, the number of reified relations \mathbf{r}_{zh} is reduced to $w \cdot v$, and all the formalisation presented in Section IV remains consistent if the zsh -th combination is replaced with the zh -th.

This simplification reduces the amount of scenes features that the algorithm exploits to bootstrap the memory graph, which becomes less intelligible. Also, this simplification can lead to *singularities*, which occur when two different scenes are encoded with the same beliefs. In general, singularities occur when an input interface does not capture the scene features relevant for the application, but this simplification aggravates such an issue because Γ_s is disregarded even if it might refer to a characteristic feature of the scene.

Algorithm 1 The fuzzy SIT algorithm.

Prior Knowledge: v element types Γ , and w relations \mathbf{r} .
State: a fuzzy ontology \mathcal{O} with the related reasoner.
Constants: the membership threshold $\text{th}_m \in [0, 1]$ the similarity threshold $\text{th}_s \geq 0$, and the fuzziness value $a \in [0, 1]$.
Input: a set of facts F_t representing the current scene as in (1).
Output: the classification graph M_t^* as defined in (8).

▷ Encode facts of the current scene into beliefs. ◁

```

1:  $d_{\epsilon_t} \leftarrow 0$ 
2:  $B \leftarrow \mathcal{E}(F)$  ▷ Map the beliefs of the scene computing (4) based on (11).
3: for each  $\langle \mathbf{r}_{zh}, c_{zh} \rangle \in B$  do
4:    $\mathcal{O}.\text{assert}(\langle \langle \epsilon_t, c_{zh} \rangle : \mathbf{r}_{zh}, 1 \rangle)$    ▷ Define the scene  $\epsilon_t$  in  $\mathcal{O}$ .
5:    $d_{\epsilon_t} \leftarrow d_{\epsilon_t} + c_{zh}$ 
6: end for

   ▷ Classify the scene into categories. ◁
7:  $M_t \leftarrow \mathcal{O}.\text{query}(\Phi_j \sqsubseteq \Phi)$    ▷ Get all sub classes of  $\Phi$  in  $\mathcal{O}$ .
8:  $M_t^* \leftarrow \mathcal{C}(M_t, B_t)$    ▷ Reason on  $\mathcal{O}$  to query  $p^{\epsilon_t : \Phi_j} > 0$  as in (8).
9: for each  $\Phi_j \in M_t^*$  do
10:   $d^{\Phi_j} \leftarrow \sum_{\mathbf{r}_{zh}} k_{zh}$ 
11:   $M_t^*.\text{setSimilarity}(\Phi_j, d^{\Phi_j} / d_{\epsilon_t})$    ▷ Assign  $d_{\epsilon_t}^{\Phi_j}$  to  $\Phi_j$  (9).
   ▷ Line 8 also assigns the membership degrees  $p^{\epsilon_t : \Phi_j}$  to each  $\Phi_j$ .
12: end for

   ▷ Eventually, learn and structure a new scene category from beliefs. ◁
13: if  $\max_{\Phi_j} M_t^* \{p^{\epsilon_t : \Phi_j}\} < \text{th}_m$  or  $\max_{\Phi_j} M_t^* \{d_{\epsilon_t}^{\Phi_j}\} < \text{th}_s$  then
14:   $\Phi_t \leftarrow \mathcal{L}(B, a)$    ▷ Define a new scene category as in (5).
15:   $M_t \leftarrow \mathcal{S}(M_t, \Phi_t)$    ▷ Update  $\mathcal{O}$  and query  $\Phi_t \sqsubseteq \Phi_j$  as in (7).
16:  compute Lines 8–12   ▷ Update the classification of  $\epsilon_t$  in  $M_t^*$ .
17: end if

18:  $\mathcal{O}.\text{remove}(\epsilon_t)$    ▷ Clean all the beliefs of the scene in  $\mathcal{O}$ .
19: return  $M_t^*$ 

```

Nevertheless, the singularities that this simplification would introduce are avoided when the input interface involves *inverse* relations \mathbf{r}_z^{-1} , e.g., front and behind. Hence, this simplification might increase w , and $2w \cdot v$ combinations occur, in the worst case. With inverse relations, the information $\gamma_x : \Gamma_s$ that this simplification disregards from the fact $\langle \langle \gamma_x, \gamma_y \rangle : \Gamma_z, p_{iz} \rangle$, would be considered in $\langle \langle \gamma_y, \gamma_x \rangle : \Gamma_z^{-1}, p_{iz}^{-1} \rangle$. If *symmetric* relations are also considered, i.e., $p_{iz}^{-1} = p_{iz}$, then the beliefs would have balanced relations between inverse pairs of elements.

G. Implementation

Algorithm 1 implements the simplification presented in Section IV-F, and it provides a classification graph M_t^* given the facts F_t describing an input scene. The algorithm requires a DL reasoner able to process a fuzzy ontology \mathcal{O} , which encodes the symbols related to types Γ and relations \mathbf{r} . We rely on a constant fuzziness value a , and on two thresholds to evaluate the classification confidence. When the confidence is low, we learn and structure a new node of the memory graph from facts, which will be used to classify future input scenes.

At Lines 1–6, the algorithm performs the encoding phase to assert the beliefs that represent the current scene ϵ_t in \mathcal{O} . At Lines 7–12, the memory graph M is retrieved by querying all the subclasses of Φ from \mathcal{O} , and M_t^* is classified by selecting only the categories $\Phi_j \sqsubseteq \Phi$ having ϵ_t as their instance, i.e., when $p^{\epsilon_t : \Phi_j} > 0$. In addition, the similarity value $d_{\epsilon_t}^{\Phi_j}$ is computed and associated to each category of M_t^* , which also encodes the membership value $p^{\epsilon_t : \Phi_j}$ computed by FuzzyDL.

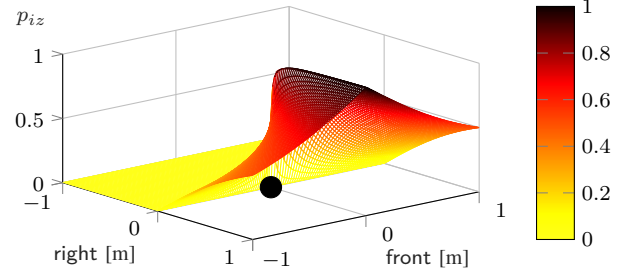


Figure 3. The fuzzy kernel defining a $\langle \langle \gamma_x, \gamma_y \rangle : \text{front}, p_{iz} \rangle$ axiom (1). Given an *element* of interest γ_x located in $(0,0)$, the kernel provides the degree p_{iz} based on the relative position of the γ_y element. The kernel is oriented based on a global reference frame to discriminate front and right relations.

Line 13 assesses the confidence of the classification by considering the nodes that classify ϵ_t with the highest membership and similarity values. Indeed, if $p^{\epsilon_t : \Phi_j}$ is lower than a threshold, then the scene beliefs do not enough respect cardinality restrictions, while, if $d_{\epsilon_t}^{\Phi_j}$ is too low, the classification would regard only a small portion of the scene ϵ_t . If one of these cases occurs, Line 14 is used to learn a new scene category Φ_t through \mathcal{L} . At Line 15, Φ_t is structured by \mathcal{S} in the memory graph M that is represented in the ontology \mathcal{O} .

Line 16 reclassifies the inputs with the new memory graph M . Hence, the returned M_t^* always contains at least a node Φ_j and, if it has just been learned, it would have $d_{\epsilon_t}^{\Phi_t} = 1$, and $p^{\epsilon_t : \Phi_t} = 1$ by construction. Line 18 removes all the encoded beliefs in the ontology for processing future input scenes.

V. FUZZY SIT EVALUATION

A. Evaluation Methodology

We considered a scenario where the robot is a passive observer that acquires point clouds of tabletop scenes where objects are arranged by a user. At each arranged scene, Algorithm 1 is computed and the outcomes are inspected. We aim to evaluate the memory graphs that fuzzy SIT bootstraps and the scene classification that it performs. Section V-B describes the semantic of the scenes, which are defined with an input interface encoding scenes in terms of objects shapes and their spatial relations.

Section V-C focusses on the memory graph bootstrapped from a few demonstrations. Since we want to compare SIT in the fuzzy and crisp domains, we replicated the scenes (shown in Figures 4a–4e) used in [7] to evaluate the crisp implementation of SIT based on a similar input interface. Since the crisp SIT is not robust to small input changes, in [40], we proposed a dialogue-based supervision step to assure input correctness. In this paper instead, we avoid the supervision step and we provide fuzzy SIT with input facts affected by perception noise. Hence, we investigate the amount of vagueness that the fuzzy SIT can handle, while expecting to bootstrap memory graphs consistent with the crisp domain.

Section V-D presents another evaluation, which focusses on the robustness of fuzzy SIT by considering the classification distribution under noisy input facts. We expect such a distribution to be smooth with respect to slightly different input facts, and that fuzzy SIT can consistently classify similar scenes.

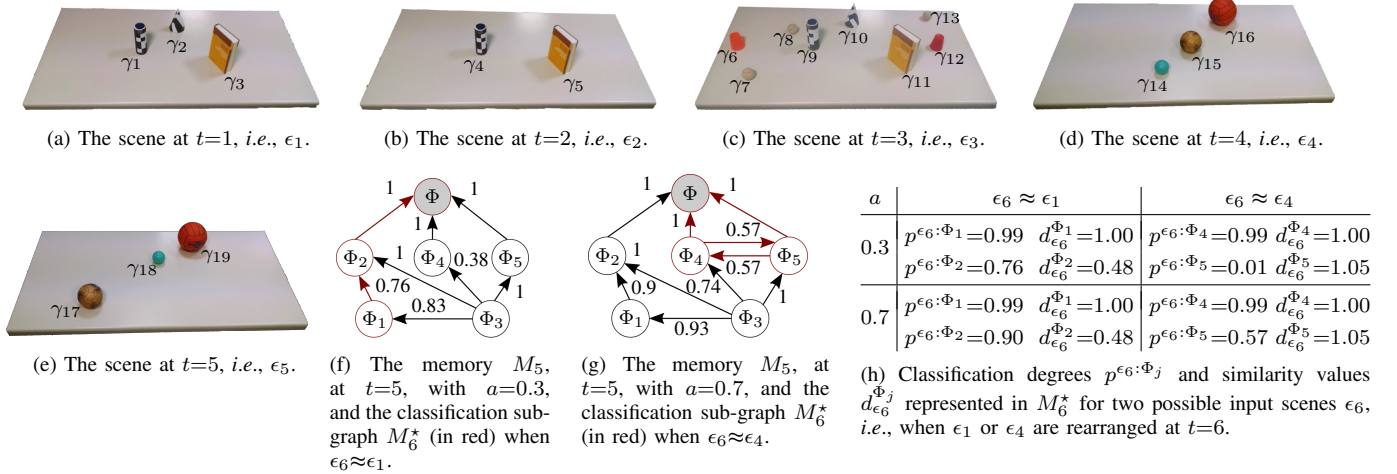


Figure 4. Scenes perceived as noisy symbolic facts over time, the representation that fuzzy SIT bootstrapped, and the classification of new scenes. Figures (a)–(e) shows a sequence of scenes ϵ_t that had been consequently learned as categories Φ_t . Scene categories were structured in the memory graph M_t for different fuzziness values as shown in (f) $a=0.3$, and (g) $a=0.7$. The graph (f) also highlights the classification sub-graph M_6^* obtained when ϵ_1 (a) was arranged again but with small differences (i.e., $\epsilon_6 \approx \epsilon_1$) at $t=6$, while (g) highlights M_6^* when a new scene $\epsilon_6 \approx \epsilon_4$ was rearranged. Table (h) details the fuzzy classification degrees $p^{\epsilon_6:\Phi_j}$ and similarity values $d_{\epsilon_6}^{\Phi_j}$ that was encoded in the j -th nodes of M_6^* with the two possible new scenes ϵ_6 . Since ϵ_6 was always classified with high values in some Φ_j , no category Φ_6 have been learned at $t=6$, i.e., M_6 had the same structure of M_5 .

Finally, Section V-E compares the complexity of fuzzy SIT among different sizes of the memory graph and input interface.

B. Experimental Setup: an Input Interface Designing

In our evaluations, we design an input interface concerning objects as scene elements (γ_x, γ_y) , their shape as their types (Γ_s, Γ_h) , and their mutual spatial relations r_z (1). In particular, we configure prior knowledge in the input interface to encompass $\Gamma \sqsubseteq \{\text{SPHERE, CONE, CYLINDER, PLANE}\}$, and $r \sqsubseteq \{\text{front, right, behind, left}\}$, which involve inverse and symmetric pairs of relations.

We perceive the shapes of objects from point cloud using RANSAC, and we identify a confidence value based on the ratio of the points of an object that match a given shape, which accuracy is reported in [46]. Differently from the crisp domain, we do not assign to an object the shape with the highest confidence. Instead, an object can be of different shapes simultaneously, with fuzzy degrees p_{is} (or p_{ih}) (1) associated to the related confidences.

The perception pipeline proposed in [46] was also used to perceive the centre of mass of each objects, which has been projected in the 2D plane associated with the workbench. In the crisp SIT, spatial relations are identified through threshold-based rules involving pair of centre of mass [7]. Instead, in this paper we exploit fuzzy kernels as in [47], and Figure 3 shows the kernel to compute the degree of front relations. The kernel is centred on an object of interest γ_x and defines a fuzzy degree p_{iz} (1) based on the relative position of another object γ_y . The right kernel is obtained with a rotation of $\pi/2$ with respect to a global reference frame placed on the workbench, and a similar rotation define behind and left as inverse and symmetric.

C. Scenes Bootstrapping

When Algorithm 1 processed the ϵ_t scenes over time instants t (as shown in Figures 4a–4e), it learned a scene category Φ_t for each ϵ_t , and the final structured memory was the graph shown in Figure 4f when $a=0.3$, and Figure 4g when $a=0.7$. Figure 4 shows that both memory graphs bootstrapped with fuzzy SIT have a logic representation consistent with the one obtained with the crisp SIT [7] deployed in the same scenario.

In particular, at $t=1$, we consider an empty memory graph M_0 , and we encoded the beliefs related to ϵ_1 . Since no classification could occur, the category Φ_1 was structured as a node of the memory graph M_1 . The node only subsumed the root Φ with degree 1 due to the definition of \mathcal{L} (5).

At $t=2$, we perceived the input facts relate to the ϵ_2 scene, where the γ_4 object was also classified as a CONE, and the centres of mass of each object was nosily perceived. We report in (12) the input facts F_2 that we observed, whereas the relative beliefs encoded through \mathcal{E} (4) are shown in (13).

$$\begin{aligned} &\langle \gamma_4:\text{CONE}, 0.82 \rangle, \langle \gamma_4:\text{CYLINDER}, 1 \rangle, \langle \gamma_5:\text{PLANE}, 1 \rangle, \\ &\langle (\gamma_4, \gamma_5):\text{right}, 0.16 \rangle, \langle (\gamma_4, \gamma_5):\text{behind}, 0.84 \rangle. \\ &\langle (\gamma_5, \gamma_4):\text{left}, 0.16 \rangle, \langle (\gamma_5, \gamma_4):\text{front}, 0.84 \rangle. \end{aligned} \quad (12)$$

$$\begin{aligned} &(\epsilon_2, 0.17):\text{right CYLINDER}, (\epsilon_2, 0.82):\text{behind CYLINDER}, \\ &(\epsilon_2, 0.84):\text{front PLANE}, (\epsilon_2, 0.17):\text{left PLANE}, \\ &(\epsilon_2, 0.17):\text{right CONE}, (\epsilon_2, 0.84):\text{behind CONE}. \end{aligned} \quad (13)$$

Since the cardinality of ϵ_2 were not satisfied by the restrictions of Φ_1 , ϵ_2 was not classified in any category of M_1 . Thus, a new category Φ_2 was learned through \mathcal{L} (5), which defines a cardinality restriction ${}^a\Omega(c_{zh})$ for each zh -th combinations of beliefs shown in (13), with related cardinalities c_{zh} .

Then, the category Φ_2 were structured by \mathcal{S} (7) in the memory M_1 , which got update in a new hierarchy M_2 . The latter graph represents ϵ_2 as a sub-scene of ϵ_1 . In other

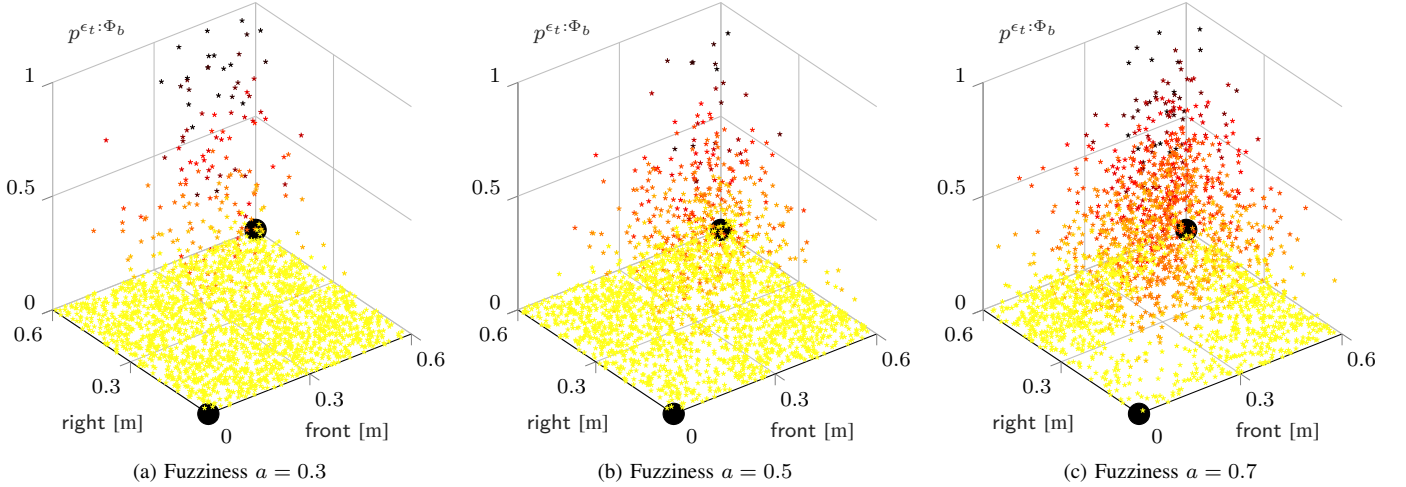


Figure 5. The fuzzy *classification degree* distribution within the scenario introduced in Figure 6. Each plot shows the classification degree $p^{\epsilon_t:\Phi_b}$ of 2500 scenes ϵ_t classified in the category Φ_b , which was learned from ϵ_b (Figure 6a). In the plots, two spheres refer to the balls shown in Figure 6, and the $p^{\epsilon_t:\Phi_b}$ degree has been drawn relatively to the position that the glass had in each ϵ_t . The plots exploit the colormap in Figure 3 and encompass different *fuzziness* values. For small fuzziness values, only very similar scenes are classified (*i.e.*, $a=0$ reduces the classification to the crisp domain) while, for high fuzziness values, this condition is more relaxed. Note that the data shown in these plots is affected by perception noise in terms of object recognition and position.

terms, FuzzyDL infers that the category Φ_1 implies Φ_2 , *i.e.*, $\Phi_1 \sqsubseteq \Phi_2$. To better appreciate this implication, let us compare Φ_2 , which is deducible from (13), and Φ_1 (14).

$$\begin{aligned}
 \Phi_1 &\triangleq \Phi \sqcap \exists \text{left CYLINDER.}^a\Omega(0.43) \sqcap \\
 &\exists \text{front CYLINDER.}^a\Omega(0.13) \sqcap \exists \text{right CYLINDER.}^a\Omega(0.35) \sqcap \\
 &\exists \text{behind CYLINDER.}^a\Omega(0.9) \sqcap \exists \text{front PLANE.}^a\Omega(0.78) \sqcap \\
 &\exists \text{left PLANE.}^a\Omega(0.72) \sqcap \exists \text{right CONE.}^a\Omega(0.94) \sqcap \\
 &\exists \text{behind CONE.}^a\Omega(1) \sqcap \exists \text{left CONE.}^a\Omega(0.43) \sqcap \\
 &\exists \text{front CONE.}^a\Omega(0.58). \quad (14)
 \end{aligned}$$

The comparison shows that $\Phi_2 \not\sqsubseteq \Phi_1$ because Φ_1 had more restriction than Φ_2 , which would never be satisfied. Instead, $\Phi_1 \sqsubseteq \Phi_2$ because Φ_1 had all zh -th combinations restricted by Φ_2 . In particular, the behind CONE, right CONE, left PLANE, behind CYLINDER, right CYLINDER cardinalities of Φ_1 were always greater than in Φ_2 ; hence, the related restrictions were satisfied (Figure 2b). Furthermore, Φ_1 had the cardinality related to the front PLANE combination lower than Φ_2 , but its value was within the range defined by the fuzziness a , *i.e.*, the restriction was fuzzy satisfied (Figure 2c).³

Accordingly with Section IV-D, fuzzy SIT used the minimum subsumption degree among zh -th combinations to identify the $p^{\Phi_1 \sqsubseteq \Phi_2}$ degree, which was the one occurring in the front PLANE combination. Thus, the graph M_2 had the root Φ and two nodes: Φ_1 and Φ_2 , which were connected with an edge starting from Φ_1 and ending in Φ_2 with a fuzzy degree $p^{\Phi_1 \sqsubseteq \Phi_2}$ that depended on the fuzziness value, as also shown in Figures 4f and 4g. The implication $\Phi_1 \Rightarrow \Phi_2$ represents that any scene classified as Φ_1 would necessary also be classified as Φ_2 . Therefore, the memory graph had more complex scenes toward its leafs, while simple configurations are closer to the root Φ , which is consistent with the behaviour of crisp SIT.

³If the cardinality related to front PLANE beliefs was not within the range specified by a (Figure 2d), then FuzzyDL would have inferred that $\Phi_1 \not\sqsubseteq \Phi_2$.

At $t=3$, we encoded ϵ_3 , which was classified in Φ_1 and Φ_2 with an high fuzzy classification degree, but low similarity value. Hence, the Line 13 of Algorithm 1 led to bootstrap a new category. We learned Φ_3 , which satisfied all the restrictions of Φ_2 , *i.e.*, $p^{\Phi_3 \sqsubseteq \Phi_2} = 1$, and fuzzy satisfied the restrictions of Φ_1 , *i.e.*, $p^{\Phi_3 \sqsubseteq \Phi_1} = 0.76$ with $a=0.3$ and $p^{\Phi_3 \sqsubseteq \Phi_1} = 0.9$ with $a=0.7$. Consequentially, a new memory M_3 were structured as $\Phi_1 \sqsubseteq \Phi_2$, $\Phi_3 \sqsubseteq \Phi_2$, $\Phi_3 \sqsubseteq \Phi_1$, with fuzzy subsumption degrees as shown in Figures 4f and 4g.

At time $t=4$, we bootstrapped the category Φ_4 in the memory M_4 , and Φ_5 was included at $t=5$ in M_5 (Figure 4). Since Φ_3 , Φ_4 and Φ_5 concerned three spheres placed in a similar configuration, Φ_4 was implied by Φ_3 in M_4 , and the same also occurred for Φ_5 in M_5 . Regardless from the used fuzziness value, Φ_1 and Φ_2 did neither imply Φ_4 nor Φ_5 .

When we used crisp SIT in the same scenario, we could not discriminate the ϵ_4 and ϵ_5 scenes. Indeed crisp SIT learned a category Φ_4 , and classified ϵ_5 in Φ_4 [7], *i.e.*, the learning and structuring mechanism at $t=5$ were not performed. In contrast, the fuzzy implementation could differentiate ϵ_4 and ϵ_5 by considering vague spatial relations rather than crisp thresholds. In particular, the bootstrapping of Φ_5 depends on the thresholds th_m and th_s used in Algorithm 1. Crisp SIT only requires th_s , which identifies the minimum similarity value $d_{\epsilon_t}^{\Phi_j}$ (9) to discriminate sub-scenes so different to require a new scene bootstrapping. Instead, fuzzy SIT also requires th_m , which concerns the minimum fuzzy classification degree $p^{\epsilon_t:\Phi_j}$ under which we learn a new category (Section IV-E).

With $a=0.3$, fuzzy SIT could not classify the scene ϵ_5 since M_3^* was empty, *i.e.*, $p^{\epsilon_5:\Phi_4}=0$, and we could not compute $d_{\epsilon_5}^{\Phi_4}$. When $a=0.7$, the classification degree was $p^{\epsilon_5:\Phi_4}=0.56$, and similarity $d_{\epsilon_5}^{\Phi_4}=0.95$. Hence, fuzzy SIT learned Φ_5 because either ϵ_5 was not classified, or because the classification degree was lower than th_m . In addition, with low fuzziness values, Φ_4 and Φ_5 were considered as distinct categories, while with high fuzziness values, the cardinality restrictions

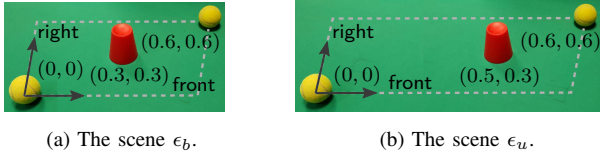


Figure 6. The scenario used to evaluate the classification distribution, where scenes are obtained by moving the glass within the rectangle having the balls as vertexes. The scene learned to compute the classification shown in Figure 5 was (a), while (b) was used to obtain the distribution shown in Figure 7.

Φ_4 and Φ_5 tends to overlap. Categories with overlapping features represent qualitatively similar scenes, and they are denoted by nodes with mutual implications, as shown in Figure 4g. When $a=0$, fuzzy SIT performed as the crisp SIT, which cannot have memory graphs with mutual implications since Algorithm 1 does not invoke the learning phase when a scene is classified. Instead, when $a=1$, mutual implications are lucky to occur since fuzzy SIT relates all cardinalities of the same zh -th combination, but with low degree. Generally, Figure 4f and 4g shows that subsumption degrees increase when the fuzziness value increases because the relative sub-scenes features overlap more.

Figure 4f and 4g also highlight the classification graphs M_6^* we obtained through \mathcal{C} (8) when we arranged again the scenes in Figure 4a or 4d at $t=6$, *i.e.*, $\epsilon_6 \approx \epsilon_1$ or $\epsilon_6 \approx \epsilon_4$, respectively. The graph M_6^* represented the classification in terms of fuzzy implications between some categories of M_6 , and its nodes encode: the cardinality restrictions (5), the similarity value $d_{\epsilon_t}^{\Phi_j}$ and the classification degree $p^{\epsilon_t:\Phi_j}$. Table 4h shows the $d_{\epsilon_t}^{\Phi_j}$ and $p^{\epsilon_t:\Phi_j}$ values encoded in the nodes of the classification graph for the two possible scenes arranged at $t=6$, and relative fuzziness values. Consistently with the crisp implementation, the similarity values identified by fuzzy SIT was high in the leafs of M_t^* and they reduced toward the root Φ . As introduced in Section IV-E, the similarity value of SIT is not linear with the number of objects in the scene, but with the number of relations. Thus, similarity comparisons are more accurate when they involve scenes with a comparable number of objects, otherwise, the differences would rapidly increase.

At $t=7$, we arranged again the scene in Figure 4c, *i.e.*, $\epsilon_7 \approx \epsilon_3$, and the classification graph M_7^* involved all the nodes shown in Figure 4f and 4g, with the relative fuzziness value. For instance, when we considered $a=0.7$, the classification degree and similarity values in M_7^* was

$$\begin{aligned} d_{\epsilon_6}^{\Phi_3} &= 1, & p^{\epsilon_6:\Phi_3} &= 0.97, & d_{\epsilon_6}^{\Phi_5} &= 0.2, & p^{\epsilon_6:\Phi_5} &= 1, \\ d_{\epsilon_6}^{\Phi_1} &= 0.29, & p^{\epsilon_6:\Phi_1} &= 0.93, & d_{\epsilon_6}^{\Phi_4} &= 0.19, & p^{\epsilon_6:\Phi_4} &= 0.74, \\ d_{\epsilon_6}^{\Phi_2} &= 0.14, & p^{\epsilon_6:\Phi_2} &= 1. \end{aligned} \quad (15)$$

It is noteworthy that $p^{\epsilon_8:\Phi_5} > p^{\epsilon_8:\Phi_4}$. This occurred because the scene in Figure 4c has three spheres more similarly placed to the category Φ_5 than Φ_4 . The classification degree depends on the overlapping between encoded beliefs and cardinality restrictions induced by the fuzziness value a . The next section also details this aspect and the differences of the similarity value in the crisp and fuzzy domains.

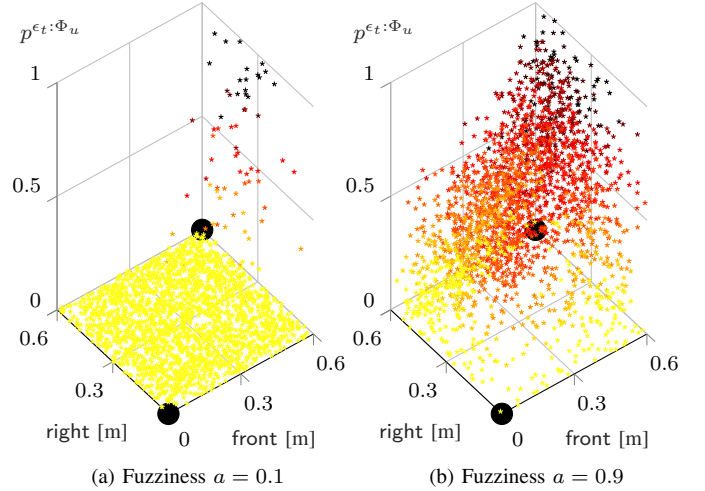


Figure 7. The classification degree distribution concerning Φ_u , *i.e.*, a category learned from ϵ_u (Figure 6b). The plots are drawn as described in Figure 5. In this case, we can note that the distribution is not centered as in Figure 5, but it changes relatively to the position of the glass in Figure 6b.

D. Classification Distributions

Let us considered a scenario where two balls (*i.e.*, SPHERE) delimit a rectangle containing a glass (*i.e.*, CYLINDER), as shown in Figure 6. In this scenario, we bootstrapped memory graphs with one category, which is learned with the glass in a specific position, *i.e.*, as shown if Figure 6a or 6b. Then, we arranged new scenes by moving the glass, and we collected their fuzzy classification degrees and similarity values with respect to the previously learned category. Figures 5 and 7 show the classification distribution where, for each position assumed by the glass, we draw the classification degree of the respective scene. For simplicity, Figures 5 and 7 also show two spheres that represent the balls on the workbench.

To collect the data shown in Figure 5, we encoded the scene ϵ_b as in Figure 6a, and we learned the scene category Φ_b

$$\begin{aligned} \Phi_b &\triangleq \Phi \sqcap \exists \text{left CYLINDER.}^a \Omega(0.74) \sqcap \\ &\exists \text{behind SPHERE.}^a \Omega(0.62) \sqcap \exists \text{right CYLINDER.}^a \Omega(0.67) \sqcap \\ &\exists \text{front CYLINDER.}^a \Omega(0.32) \sqcap \exists \text{right SPHERE.}^a \Omega(0.94) \sqcap \\ &\exists \text{behind CYLINDER.}^a \Omega(0.66) \sqcap \exists \text{left SPHERE.}^a \Omega(0.78) \sqcap \\ &\exists \text{front SPHERE.}^a \Omega(0.72). \end{aligned} \quad (16)$$

Then, we collected 2500 scenes ϵ_t with the glass in different positions, and we evaluate their classification $\epsilon_t:\Phi_b$ with a fuzziness value $a=0.3$. The same experiment was also performed with $a=0.5$ and $a=0.7$, and the relative fuzzy classification degrees $p^{\epsilon_t:\Phi_b}$ are shown in Figure 5.

When a was low, fuzzy SIT tended to its crisp implementation, and it could only classify the scenes having beliefs cardinality close to the one processed while learning Φ_b . Instead, when a was high, fuzzy SIT classified more scenes having beliefs that differ from the one used while learning Φ_b . Indeed, with $a=0.3$, only 349 scenes out of 2500 were classified with an average classification degree of 0.89 and a standard deviation of 0.1, whereas 1689 scenes were classified with an average of 0.98 and a standard deviation of 0.13

when $a=0.7$. For all the a values, fuzzy SIT classified scenes accordingly with the learned category Φ_b , and this is shown in Figures 5 since the higher classification degrees occurred when the glass was in the middle, *i.e.*, as shown in Figure 6a.

Figure 5 shows that the classification distribution increased with the fuzziness value, and this gives an intuitive reason why scene overlapped more when $a=0.7$ than $a=0.3$ in the previous scenario (Section V-C). Also, with a high a , each zh -th combinations of cardinality restrictions led to higher fuzzy degrees p_{zh} when the cardinality $c_{zh} \in (k^-, k)$, as shown in Figure 2a. Since the classification degree $p^{\epsilon_t: \Phi_b}$ is given by the fuzzy conjunction of each zh -th combination (5), higher fuzziness values allowed for a smoother transition between the degrees of scenes that are (or not) classified.

We performed the same experiment also with the scene ϵ_u shown in Figure 6b, which lead to the learned category

$$\begin{aligned} \Phi_u \triangleq & \Phi \sqcap \exists \text{left CYLINDER.}^a \Omega(0.16) \sqcap \\ & \exists \text{behind SPHERE.}^a \Omega(1.01) \sqcap \exists \text{right CYLINDER.}^a \Omega(0.72) \sqcap \\ & \exists \text{front CYLINDER.}^a \Omega(0.85) \sqcap \exists \text{right SPHERE.}^a \Omega(0.68) \sqcap \\ & \exists \text{behind CYLINDER.}^a \Omega(0.35) \sqcap \exists \text{left SPHERE.}^a \Omega(0.85) \sqcap \\ & \exists \text{front SPHERE.}^a \Omega(0.65). \end{aligned} \quad (17)$$

Figure 7 shows the classification distribution we observed with $a=0.1$ and $a=0.9$, and it highlights the effect of the fuzziness value, which was coherent with the one observed in Figure 5. Furthermore, the used input interface (described in Section V-B) were consistently able to represent the scenes characteristics. Indeed, also the distribution shown in Figure 7 show an higher classification degree in correspondence to the glass position related to Φ_u (Figure 6b).

It is noteworthy that the plots in Figure 5 and 7 show some outliers, which were due to a vague identification of the centre of mass and object type degrees. Such a noise perturbed p_{iz} and p_{ih} (1), which affect c_{zh} consequently (11). We designed the scenario shown in Figure 6 to stress the encoding facton (4) because scenes have the same zh -th combinations of beliefs, *e.g.*, (16) and (17). For maintaining this scenes characteristic, we used objects that were always perceived with the same shapes.

Figure 5 and 7 shows that the fuzziness value a could be tuned to make our algorithm robust to perception noise that generate reasonably small variances in the input facts. Indeed, the 12500 scenes ϵ_t used to perform the experiments shown in Figures 5 and 7 were subjected to noises affecting (i) the object centre of mass, with an average of 0.015m and standard deviation of 0.038m, and (ii) the fuzzy degree associate to the object shapes, with an average of 0.093 and a standard deviation of 0.195. Figures 5 and 7 confirmed that fuzzy SIT is able to classify scenes consistently with its crisp formulation also under this noisy input facts.

In the scenario shown in Figure 6, the crisp SIT would assign a similarity value $d_{\epsilon_t}^{\Phi_j} = 1$ to each scene classified in Φ_j , *i.e.*, (16) or (17). Consistently, the fuzzy SIT computed an high similarity value, *i.e.*, with average 0.977 and standard deviation of 0.147. However, as described in Section IV-E, the fuzzy similarity might exceed 1, while the crisp similarity is bounded on $[0, 1]$. In particular, $d_{\epsilon_t}^{\Phi_j} > 1$ occurred 2199 times

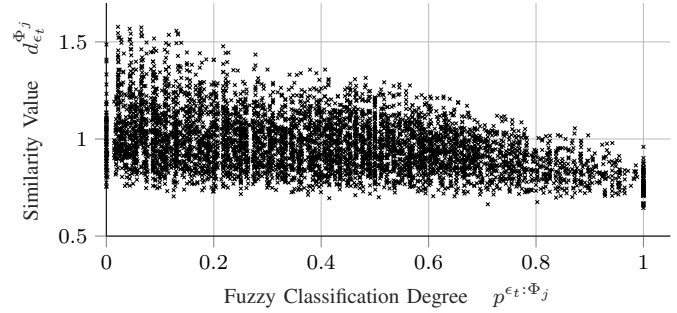


Figure 8. The *similarity* distribution with respect to the fuzzy *classification degree* among 5584 scenes arranged within the scenario shown in Figure 6.

out of 5584 classified scenes, which distribution with respect to the fuzzy classification degree $p^{\epsilon_t: \Phi_j}$ as shown in Figure 8. The latter Figure shows a linear dependence between similarity and classification degree, and that a scene classified with a high $p^{\epsilon_t: \Phi_j}$ tended not to have a similarity that exceeded 1.

In the fuzzy implementation, the similarity might exceed 1 when a zh -th combination of restriction $\Omega(k)$ was fuzzy satisfied by the related cardinality of a scene c_{zh} , *i.e.*, $k^- \leq c_{zh} \leq k$ (Figure 2a). In this case, it might be that $d^{\Phi_j} > d_{\epsilon_t}$ (9) when the scene is classified, *i.e.*, $p^{\epsilon_t: \Phi_j} > 0$. This would never occur in the crisp implementation since a scene is classified only if $c_{zh} \geq k$, *i.e.*, $d^{\Phi_j} > d_{\epsilon_t}$ always. Therefore, $p^{\epsilon_t: \Phi_j} > 1$ occurred more frequently when (i) $p^{\epsilon_t: \Phi_j}$ was low, *i.e.*, the restrictions were fuzzy satisfied, and (ii) the fuzziness a was high, *i.e.*, k^- was smaller. Nevertheless, Figure 8 shows that the similarity $d_{\epsilon_t}^{\Phi_j}$ is bounded in a range, which upper-bound depends on the used input interface and fuzziness value.

E. Computation Complexity

Figure 9 shows the computation complexity we observed with random scenes encoded through prior knowledge made by different combinations of v and w values. In other words, we changed the amount of possible symbols representing the object types Γ and relations r used to define the input interface, which spanned in $\{2, 4, \dots, 10\}$ symbols. We process 22 scenes over time, and we incrementally learned the respective categories Φ_t in the memory. In this scenario, we measured the time spent to learn and classify scenes in ontologies with a different number of axioms, *i.e.*, by modifying the number of zh -th combinations and the amount of categories in the memory. Each point in the graph is given by the average of four measurements taken within Lines 1–12 of Algorithm 1 in Figure 9a, and Lines 14–15 in Figure 9b.

We experienced an exponential increase of time when the number of axioms in the ontology increased, and this is due to FuzzyDL reasoner that is exponentially complex [8], [43]. Noteworthy, DL-based reasoning has computation time with a high variance, which is also due to the open word assumption, and to the amount of knowledge that the reasoner can infer. Thus, generalise reasoning complexity is difficult because the worst case scenario is not always representative of the typical behaviour of specific ontologies.

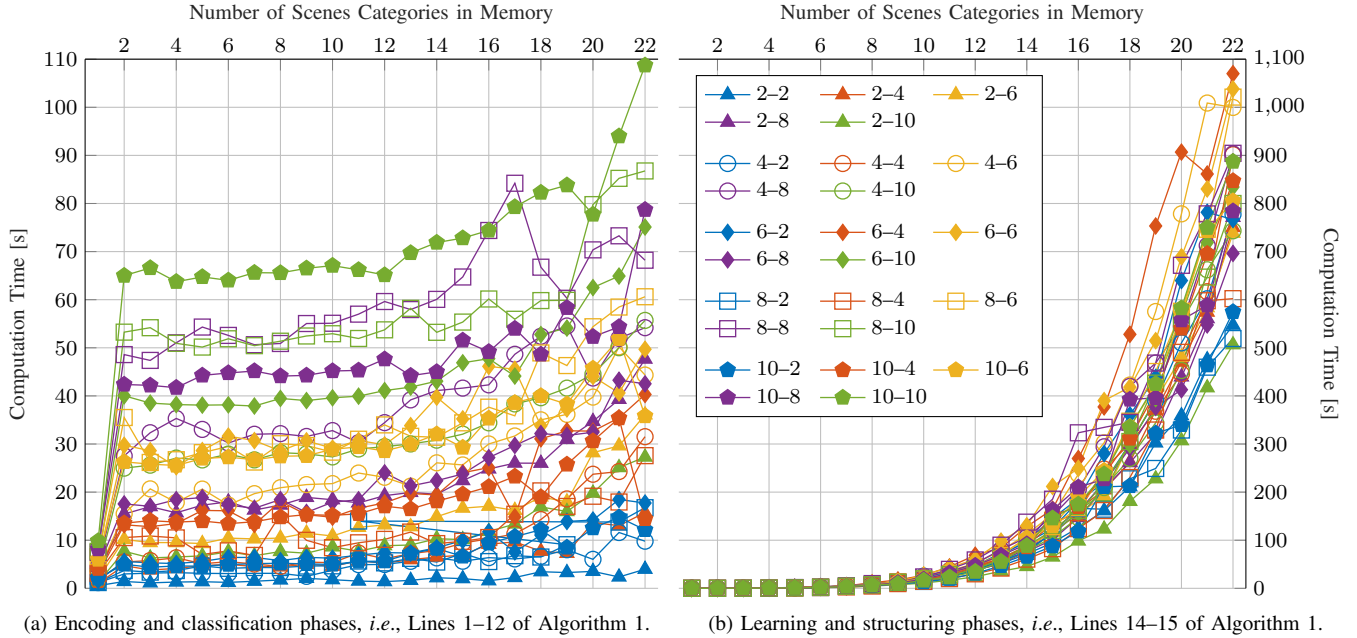


Figure 9. The computation complexity against the number of scene categories, *i.e.*, nodes, in the memory graph M . The plots are shown for different number of element types Γ and relationships r represented in the ontology as prior knowledge (1), *i.e.*, $v-w$, respectively; as shown in the legend.

Moreover, the exponential complexity introduced by the reasoner to perform the classification (8) and structuring (7) functions make the time required to perform the encoding (4) and learning (5) functions negligible. This occurs because (4) is linear with the number of facts, and (5) with the amount of zh -th combinations. Therefore, we can approximate the classification time (8) with Figure 9a, and the structuring time (7) with Figure 9b.

Figure 9 shows an exponential increase of complexity. The trend of the classification complexity (Figure 9a) is attenuated for input interfaces with a few relations v and object types w , while is aggravated for big input interfaces. However, the classification complexity was not largely affected by the number of categories in the memory. In contrast, the structuring complexity (Figure 9b) was affected by memory categories, while big input interface had a relatively small contribution.

VI. DISCUSSIONS

Section V shows that fuzzy SIT behaves consistently with its crisp counterpart since it preserves the properties concerning the encoding, learning, structuring and classification phases presented in Section IV. In particular, fuzzy and crisp SIT share the same definition of the input interface, facts and encoded beliefs. The learning function of fuzzy SIT defines scene categories through cardinality restriction as in the crisp domain. The structuring function of fuzzy and crisp SIT arrange learned scene categories in a memory graph representing sub-scene through DL-based reasoning. The classification provided by fuzzy and crisp SIT is a structure of learned categories retrieved through reasoning.

Fuzzy SIT has also additional features encompassing the following statements. (i) Elements in a scene can also be of different types at the same time, *e.g.*, CONE and CYLINDER.

(ii) Similar scenes (*e.g.*, Figures 4d and 4e) can be discriminated in the memory, and represented through implication cycles.⁴ (iii) The memory graph has edges weighed with the fuzzy subsumption degree, and (iv) the classification includes fuzzy degrees. While the crisp SIT classifies scenes with similarity values bounded in $[0, 1]$, fuzzy SIT has the drawback to compute similarities values in a range with an upper bound depending on the used input interface and fuzziness value.

Section II-B introduces the limitation of crsip SIT, which concern computation complexity and robustness to perception noises. We shown that fuzzy SIT can overcome the robustness limitations by means of the fuzziness value a . Fuzzy SIT is robust because allows a smooth transition between scene categories, while in the crisp domain there are discontinuities that lead to different scene representations even if the input facts have small differences. Such a smooth transition is also due to the definition of the input interface (1) that extends crisp axioms with fuzzy degrees. Hence, we could use fuzzy kernels (*e.g.*, Figure 3), instead of threshold-based crisp roles, and assign a confidence to the perceived object types, instead of choosing the best confident identification.

The fuzzy implementation can also deal with vague representation of scenes. This is relevant for human-robot interaction, *e.g.*, when robots and users should not share formal knowledge. Since SIT is based on a symbolic formalism, it bootstraps knowledge structures that can be intelligible to humans. However, fuzzy SIT provides information that are less intuitive than in the crisp domain because the scenes beliefs counting mechanism is less natural. Both in the crisp and fuzzy domains, the intelligibility of the knowledge bootstrapped by SIT depends on the symbols involved in the input interface,

⁴In the crisp domain the memory graph is reduced to a tree-like hierarchy.

and further works might be required for intuitively communicating them to a user. As in the crisp implementation, also fuzzy SIT allows refining learned category through interaction. Nevertheless, in contrast with our previous approach [40], fuzzy SIT is robust enough to bootstrap a scene representation without asking humans to supervise the correctness of each input fact, which involves a not negligible effort from users.

As for the crisp SIT, the intelligibility of fuzzy SIT also benefits of the incremental bootstrapping of structured representations. Indeed, having a classification of sub-scenes can help intelligibility if they have been annotated. For instance, if the user makes the robot learning a category Φ_b from the scene in Figure 6a, and if Φ_b is annotated as a *balanced* scene, the classification degrees shown in Figure 5 would rank other balanced scenes. Then, the user might bootstrap and annotate a set of relevant scene categories in the memory graph, and classify them in a more intelligible manner. This is possible thanks to the incremental bootstrapping mechanism implemented by SIT, which allows to learn and structure new categories in the memory without the need to retune the algorithm based on the categories previously bootstrapped.

The crisp and fuzzy SIT exploit a general-purpose input interface (1), which encodes some symbols as prior knowledge in the ontology to represent the elements in the scene, *i.e.*, their type and relations. Thus it requires mechanisms to perceive fuzzy degrees related to such symbols from sensors. In addition, since SIT bootstraps the memory and classify future scenes based combination of symbols provided in the input interface (*e.g.*, connectedCABLE), it can provide suitable outcomes only when the input interface allows representing the scene characteristics that are relevant for an application.

For instance, in the geometric scenarios presented in Section V, we considered a symmetric input interface designed to avoid singularities, as discussed in Sections IV-F and V-B. It is noteworthy that the input interface of SIT is not limited to the geometric domain, *e.g.*, rooms characteristics might be used to bootstrap a topology for navigating robots, or temporal events might be used to segment a human-lead demonstrative task. However, while crisp SIT only requires to ground symbols from sensor based on the input interface, fuzzy SIT also require to identify fuzzy degrees, which might involve challenging issues in some applications. Also, it is always possible to extend the input interface by considering more combinations of beliefs, *e.g.*, in BIG CONTAINER. This approach would lead to bootstrapped representations that are more expressive, but it strongly affects computation performances.

Since both crisp and fuzzy SIT exploit DL-based reasoner, which held most of the computation load, the two implementation has a comparable computation complexity. In particular, SIT scales exponentially with the amount of axioms in the ontology, which depends on the number of symbols encoded in the input interface, and on the size of the memory graph. Thus, reducing the computation load is a crucial issue for human-robot interaction. A possibility is to segment a complex application into a set of smaller domains, each with a dedicated input interface, which encompass smaller ontologies orchestrated by a semantic network, *e.g.*, as proposed in [48].

Algorithm 1 is configured to learn each scene it could

not classify. While this is suitable for specific applications (*e.g.*, when SIT can be enabled and disabled based on user inputs), it might lead to bootstrapped memory graphs unnecessary big, *e.g.*, in a long-term interaction. An approach to limit this issue, and decrease the computation load, is to assign a score to each learned category, which can be consolidated over time for maintaining in the memory only relevant categories, while the others would be forgotten. We presented a framework for evaluating different heuristics to consolidate and forget scene categories in [49], [50]. Another approach could be to periodically evaluate the memory graph in order to simplify it by reasoning on the similarity among scene categories, which are represented as fuzzy subsumption degrees.

VII. CONCLUSION

We presented a fuzzy extension of the SIT algorithm, which incrementally bootstraps structured scenes representation encompassing sub-scenes and similar scenes in an OWL-DL ontology. We shown that our extension is consistent with the crisp formulation of SIT, and it provides further features as well. Differently from crisp SIT, fuzzy SIT is robust to perception noise, and it can process sensory data in realistic setups. However, fuzzy SIT bootstraps scenes representations that are less intelligible than the one obtained with its crisp counterpart.

In particular, fuzzy SIT bootstraps a memory graph by learning from not annotated observations over time. When a new scene is observed, SIT classifies it and provide a graph representing scenes previously observed, that encodes similarity and implication measurements. The memory bootstrapped by fuzzy SIT is based on a general-purpose input interface, which can be used to represent scenes with different semantics.

The main limitation of the SIT algorithm is the computation load held by the OWL-DL reasoner. As further work we aim to address this limitation with the approaches proposed in Section VI.

REFERENCES

- [1] Y. Breux, S. Druon, and R. Zapata, "From perception to semantics: An environment representation model based on human-robot interactions," in *2018 27th IEEE International Symposium on Robot and Human Interactive Communication (RO-MAN)*, 2018, pp. 672–677.
- [2] L. Villamar Gómez and J. Miura, "Ontology-based knowledge management with verbal interaction for command interpretation and execution by home service robots," *Robotics and Autonomous Systems*, vol. 140, p. 103763, 2021. [Online]. Available: <https://www.sciencedirect.com/science/article/pii/S0921889021000488>
- [3] S. Manzoor, Y. G. Rocha, S.-H. Joo, S.-H. Bae, E.-J. Kim, K.-J. Joo, and T.-Y. Kuc, "Ontology-based knowledge representation in robotic systems: A survey oriented toward applications," *Applied Sciences*, vol. 11, no. 10, 2021. [Online]. Available: <https://www.mdpi.com/2076-3417/11/10/4324>
- [4] F. Zhang, Z. Ma, Y. Lv, and X. Wang, "Formal semantics-preserving translation from fuzzy er model to fuzzy owl dl ontology," in *2008 IEEE/WIC/ACM International Conference on Web Intelligence and Intelligent Agent Technology*, vol. 1, 2008, pp. 503–509.
- [5] J. K. Benjamin, B. Patrick, M. Joseph, and P. Jefferson, "Bootstrap learning of foundational representations," *Connection Science*, vol. 18, no. 2, pp. 145–158, 2006. [Online]. Available: <https://doi.org/10.1080/09540090600768484>
- [6] S. Coradeschi, A. Loutfi, and B. Wrede, "A short review of symbol grounding in robotic and intelligent systems," *KI-Künstliche Intelligenz*, vol. 27, no. 2, pp. 129–136, 2013. [Online]. Available: <https://doi.org/10.1007/s13218-013-0247-2>

- [7] L. Buoncompagni and F. Mastrogiovanni, "Teaching a robot how to spatially arrange objects: Representation and recognition issues," in *2019 28th IEEE International Conference on Robot and Human Interactive Communication (RO-MAN)*, 2019, pp. 1–8.
- [8] F. Baader, I. Horrocks, C. Lutz, and U. Sattler, *Introduction to Description Logic*. Cambridge University Press, Apr. 2017.
- [9] L. Xie, F. Lee, L. Liu, K. Kotani, and Q. Chen, "Scene recognition: A comprehensive survey," *Pattern Recognition*, vol. 102, p. 107205, 2020. [Online]. Available: <https://www.sciencedirect.com/science/article/pii/S003132032030011X>
- [10] Y. Gu, Y. Wang, and Y. Li, "A survey on deep learning-driven remote sensing image scene understanding: Scene classification, scene retrieval and scene-guided object detection," *Applied Sciences*, vol. 9, no. 10, 2019. [Online]. Available: <https://www.mdpi.com/2076-3417/9/10/2110>
- [11] J. Yuan, H. Abdul-Rashid, and B. Li, "A survey of recent 3d scene analysis and processing methods," *Multimedia Tools and Applications*, vol. 80, pp. 19491–19511, 2021.
- [12] M. Li, A. G. Patil, K. Xu, S. Chaudhuri, O. Khan, A. Shamir, C. Tu, B. Chen, D. Cohen-Or, and H. Zhang, "Grains: Generative recursive autoencoders for indoor scenes," *ACM Trans. Graph.*, vol. 38, no. 2, feb 2019. [Online]. Available: <https://doi.org/10.1145/3303766>
- [13] R. M. French, "Catastrophic forgetting in connectionist networks," *Trends in Cognitive Sciences*, vol. 3, no. 4, pp. 128–135, 1999. [Online]. Available: <https://www.sciencedirect.com/science/article/pii/S1364661399012942>
- [14] R. Dwivedi, D. Dave, H. Naik, S. Singhal, R. Omer, P. Patel, B. Qian, Z. Wen, T. Shah, G. Morgan, and R. Ranjan, "Explainable ai (xai): Core ideas, techniques, and solutions," *ACM Comput. Surv.*, vol. 55, no. 9, jan 2023. [Online]. Available: <https://doi.org/10.1145/3561048>
- [15] C. hua Liao, Y. fen Wu, and G. hua King, "Research on learning OWL ontology from relational database," *Journal of Physics: Conference Series*, vol. 1176, p. 022031, mar 2019. [Online]. Available: <https://doi.org/10.1088/1742-6596/1176/2/022031>
- [16] A. Cropper, S. Dumančić, R. Evans, and S. H. Muggleton, "Inductive logic programming at 30," *Machine Learning*, vol. 111, no. 1, pp. 147–172, 2022.
- [17] F. A. Lisi and U. Straccia, "A logic-based computational method for the automated induction of fuzzy ontology axioms," *Fundamenta Informaticae*, vol. 124, no. 4, pp. 503–519, 2013.
- [18] G. Rizzo, N. Fanizzi, C. d'Amato, and F. Esposito, "Approximate classification with web ontologies through evidential terminological trees and forests," *International Journal of Approximate Reasoning*, vol. 92, pp. 340–362, 2018. [Online]. Available: <https://www.sciencedirect.com/science/article/pii/S0888613X17301019>
- [19] N. Fanizzi, C. d'Amato, and F. Esposito, "Induction of robust classifiers for web ontologies through kernel machines," *Journal of Web Semantics*, vol. 11, pp. 1–13, 2012. [Online]. Available: <https://www.sciencedirect.com/science/article/pii/S1570826811000837>
- [20] M. Zhu, Z. Gao, J. Z. Pan, Y. Zhao, Y. Xu, and Z. Quan, "Tbox learning from incomplete data by inference in belnet+," *Knowledge-Based Systems*, vol. 75, pp. 30–40, 2015. [Online]. Available: <https://www.sciencedirect.com/science/article/pii/S0950705114003967>
- [21] J. Lehmann, "Hybrid learning of ontology classes," in *Machine Learning and Data Mining in Pattern Recognition*. Berlin, Heidelberg: Springer Berlin Heidelberg, 2007, pp. 883–898.
- [22] M. Nickles and A. Rettinger, "Interactive relational reinforcement learning of concept semantics," *Machine learning*, vol. 94, no. 2, pp. 169–204, 2014.
- [23] J. Potoniec, "Mining cardinality restrictions in owl," *Foundations of Computing and Decision Sciences*, vol. 45, no. 3, pp. 195–216, 2020. [Online]. Available: <https://doi.org/10.2478/fcds-2020-0011>
- [24] I. Qasim, M. Alam, S. Khan, A. W. Khan, K. M. Malik, M. Saleem, and S. A. C. Bukhari, "A comprehensive review of type-2 fuzzy ontology," *Artificial Intelligence Review*, vol. 53, no. 2, pp. 1187–1206, 2020.
- [25] F. Bobillo and U. Straccia, "fuzzydl: An expressive fuzzy description logic reasoner," in *2008 IEEE International Conference on Fuzzy Systems (IEEE World Congress on Computational Intelligence)*, 2008, pp. 923–930.
- [26] G. Stoilos, N. Simou, G. Stamou, and S. Kollias, "Uncertainty and the semantic web," *IEEE Intelligent Systems*, vol. 21, no. 5, pp. 84–87, 2006.
- [27] F. Bobillo, M. Delgado, and J. Gómez-Romero, "Delorean: A reasoner for fuzzy owl 2," *Expert Systems with Applications*, vol. 39, no. 1, pp. 258–272, 2012. [Online]. Available: <https://www.sciencedirect.com/science/article/pii/S095741741100978X>
- [28] V. Haarslev, H.-I. Pai, and N. Shiri, "Optimizing tableau reasoning in alc extended with uncertainty," in *Description Logics*, 2007.
- [29] H. Habiballa, "Resolution strategies for fuzzy description logic," in *EUSFLAT Conference (2)*. Citeseer, 2007, pp. 27–36.
- [30] U. Straccia, "A minimal deductive system for general fuzzy rdf," in *Web Reasoning and Rule Systems*. Berlin, Heidelberg: Springer Berlin Heidelberg, 2009, pp. 166–181.
- [31] D. Tsatsou, S. Dasiopoulou, I. Kompatsiaris, and V. Mezaris, "Lifir: A lightweight fuzzy dl reasoner," in *The Semantic Web: ESWC 2014 Satellite Events*. Springer International Publishing, 2014, pp. 263–267.
- [32] I. Huitzil, U. Straccia, N. Díaz-Rodríguez, and F. Bobillo, "Datil: Learning fuzzy ontology datatypes," in *Information Processing and Management of Uncertainty in Knowledge-Based Systems. Theory and Foundations*. Springer International Publishing, 2018, pp. 100–112.
- [33] F. A. Cardillo and U. Straccia, "Fuzzy owl-boost: Learning fuzzy concept inclusions via real-valued boosting," *Fuzzy Sets and Systems*, vol. 438, pp. 164–186, 2022, fuzzy and Neurofuzzy Models. [Online]. Available: <https://www.sciencedirect.com/science/article/pii/S0165011421002426>
- [34] F. Bobillo and J. Gómez-Romero, "Spatial reasoning with fuzzy ontologies," *17th International Conference on Information Processing and Management of Uncertainty in Knowledge-Based Systems (IPMU)*, 2018.
- [35] A. Tejada-Mesias, I. Dongo, Y. Cardinale, and J. Diaz-Amado, "Odrom: Object detection and recognition supported by ontologies and applied to museums," in *2021 XLVII Latin American Computing Conference (CLEI)*, 2021, pp. 1–10.
- [36] A. I. Salaou and A. Ghomari, "Fuzzy ontology-based complex and uncertain video surveillance events recognition," in *2021 International Conference on Information Systems and Advanced Technologies (ICISAT)*, 2021, pp. 1–5.
- [37] Y. Zheng, Z. Xu, and X. Wang, "The fusion of deep learning and fuzzy systems: A state-of-the-art survey," *IEEE Transactions on Fuzzy Systems*, vol. 30, no. 8, pp. 2783–2799, 2022.
- [38] M. Yeganejou, S. Dick, and J. Miller, "Interpretable deep convolutional fuzzy classifier," *IEEE Transactions on Fuzzy Systems*, vol. 28, no. 7, pp. 1407–1419, 2020.
- [39] M. Kulmanov, F. Z. Smali, X. Gao, and R. Hoehndorf, "Semantic similarity and machine learning with ontologies," *Briefings in Bioinformatics*, vol. 22, no. 4, 10 2020. [Online]. Available: <https://doi.org/10.1093/bib/bbaa199>
- [40] L. Buoncompagni and F. Mastrogiovanni, "Dialogue-based supervision and explanation of robot spatial beliefs: a software architecture perspective," in *2018 27th IEEE International Symposium on Robot and Human Interactive Communication (RO-MAN)*, 2018, pp. 977–984.
- [41] L. Buoncompagni, F. Mastrogiovanni, and A. Saffiotti, "Scene Learning, Recognition and Similarity Detection in a Fuzzy Ontology via Human Examples," in *Proceedings of the 4th Italian Workshop on Artificial Intelligence and Robotics*, vol. 2054. Bari, Italy: CEUR-WS, nov 2017, pp. 10–15.
- [42] B. Motik, P. F. Patel-Schneider, and B. Parsia, "OWL 2 Web Ontology Language Structural Specification and Functional-Style Syntax (Second Edition)," World Wide Web Consortium (W3C), Tech. Rep., December 2012, <https://www.w3.org/TR/owl2-syntax/>.
- [43] F. Bobillo and U. Straccia, "The fuzzy ontology reasoner fuzzyDL," *Knowledge-Based Systems*, vol. 95, pp. 12–34, 2016.
- [44] —, "On Qualified Cardinality Restrictions in Fuzzy Description Logics under Łukasiewicz semantics," in *Proceedings of the 12th International Conference of Information Processing and Management of Uncertainty in Knowledge-Based Systems (IPMU 2008)*, vol. 8, jun 2008, pp. 1008–1015.
- [45] J. Chamorro-Martínez, D. Sánchez, J. M. Soto-Hidalgo, and P. M. Martínez-Jiménez, "A discussion on fuzzy cardinality and quantification. Some applications in image processing," *Fuzzy Sets and Systems*, vol. 257, pp. 85–101, Dec. 2014.
- [46] L. Buoncompagni and F. Mastrogiovanni, "A software architecture for object perception and semantic representation," in *Proceedings of the 2nd Italian Workshop on Artificial Intelligence and Robotics A workshop of the XIV International Conference of the Italian Association for Artificial Intelligence (AI²IA)*, vol. 1544. CEUR-WS, 2015, pp. 116–124.
- [47] L. Buoncompagni, S. Ghosh, M. Moura, and F. Mastrogiovanni, "A scalable architecture to design multi-modal interactions for qualitative robot navigation," in *XVII International Conference of the Italian Association for Artificial Intelligence (AI²IA) – Advances in Artificial Intelligence*. Springer International Publishing, 2018, pp. 96–109.
- [48] L. Buoncompagni, S. Y. Kareem, and F. Mastrogiovanni, "Human activity recognition models in ontology networks," *IEEE Transactions on Cybernetics*, pp. 1–20, 2021.

- [49] L. Buoncompagni and F. Mastrogiovanni, “A framework inspired by cognitive memory to learn planning domains from demonstrations,” in *Proceedings of the 6th Italian Workshop on Artificial Intelligence and Robotics co-located with the XVIII International Conference of the Italian Association for Artificial Intelligence (AIxIA)*, vol. 2594. CEUR-WS, 2019, pp. 13–18.
- [50] —, “Learning symbolic task representation from a human-led demonstration: A memory to store, retrieve, consolidate, and forget experiences,” *arXiv*, vol. 2404.10591, 4 2024. [Online]. Available: <https://arxiv.org/abs/2404.10591>